Nocturnal Blood Glucose and IGFBP-1 Changes in Type 1 Diabetes: Differences in the Dawn Phenomenon between Insulin Regimens

Authors

H. Yagasaki[1], K. Kobayashi[1], T. Saitou[1], K. Nagamine[1], Y. Mitsui[1], M. Mochizuki[1], K. Kobayashi[1], H. Cho[2], K. Ohyama[1], S. Amemiya[3], S. Nakazawa[1]

Affiliations

[1] Department of Pediatrics, Faculty of Medicine, University of Yamanashi, Yamanashi, Japan
[2] Department of Pediatrics, Kawasaki Municipal Hospital, Kanagawa, Japan
[3] Department of Pediatrics, Faculty of Medicine, Saitama Medical School, Saitama, Japan

Key words
- insulin-like growth factor binding protein-1
- dawn phenomenon
- type 1 diabetes mellitus

Abstract

Objective: Insulin-like growth factor binding protein-1 (IGFBP-1) is known to regulate the bioavailability of insulin-like growth factor (IGF) and the levels of IGFBP-1 are increased in the morning in patients with type 1 diabetes mellitus. We investigated the nocturnal fluctuations of glucose, IGFBP-1, and free IGF-1 levels with three insulin regimens.

Research Design and Methods: Forty-eight type 1 diabetes patients were divided into three groups according to their basal insulin therapy (continuous subcutaneous insulin infusion [CSII], insulin glargine, NPH insulin). Blood samples were obtained every 2 h between 2300 h and 0700 h to measure plasma glucose, IGFBP-1 and free IGF-1 levels.

Results: The dawn phenomenon was more frequent with NPH (62.1%) than with glargine (16.6%, $p<0.05$) and CSII (14.3%, $p<0.05$). In the NPH group, the serum IGFBP-1 levels were markedly increased from 21.0±3.6 ng/ml at 2300 h to 200.3±21.8 ng/ml at 0700 h and free IGF-1 levels were inversely decreased; these changes were partially suppressed in the CSII and glargine groups.

Conclusions: The use of insulin regimens that provide sufficient insulin levels in the early morning can suppress the dawn phenomenon, leading to improved glycemic control. The increase in circulating IGFBP-1 in the morning, as a result of waning of insulin action, lowers free IGF-1 levels and may cause insulin resistance.

received 14.06.2009
first decision 05.08.2009
accepted 24.08.2009

Bibliography
DOI http://dx.doi.org/10.1055/s-0029-1239518
Published online: October 15, 2009
Exp Clin Endocrinol Diabetes 2010; 118: 195–199

ISSN 0947-7349

Correspondence
H. Yagasaki, MD
Department of Pediatrics
Faculty of Medicine University of Yamanashi
1110 Shimokato, Chuo
409-3898 Yamanashi
Japan
Tel.: +81 55-273-9606
Fax: +81 55-273-6745
yagasaki@mwd.biglobe.ne.jp

Introduction

Patients with type 1 diabetes mellitus are in an insulin-deficient state due to pancreatic β-cell dysfunction. Therefore, they need insulin replacement therapy, which is predominantly achieved via subcutaneous injection of recombinant insulin. However, nocturnal hypoglycemia is one of the limiting factors for strict insulin treatment, because severe hypoglycemia often causes neurological outcomes such as convulsion or neuropsychological dysfunction. Because of this fear of nocturnal hypoglycemia, patients are often unwilling to inject the appropriate dose of insulin, and thus experience insulin insufficiency in the early morning because of the early waning of insulin activity. Because of this fear of nocturnal hypoglycemia, patients often decrease their insulin doses at bedtime and thus experience insulin insufficiency in the early morning.

The dawn phenomenon was first reported in 1981 (Schmidt et al., 1981) and is characterized by a marked increase in glucose levels in the morning (dawn), which is caused by a combination of the waning of the insulin (commonly NPH insulin) injected the previous night in addition to an increase in insulin resistance, which has been demonstrated by the glucose clamp method (van Cauter et al., 1989). The onset of insulin resistance at dawn is believed to be due to nocturnal surges of counterregulatory hormones such as growth hormone (Perriello et al., 1990). In addition, Kobayashi et al. reported that IGF binding protein (IGFBP)-1 also plays a role in nocturnal glycemic control (Kobayashi et al., 1997).

IGFBP-1 is produced mainly in the liver and its transcription is inhibited by insulin. Thus, IGFBP-1 and insulin both play important roles in the regulation of short-term IGF-1 bioavailability (Lee et al., 1997; Lang et al., 2003). The levels of IGFBP-1 fluctuate with a peak before breakfast, and patients with type 1 diabetes often show extremely high IGFBP-1 levels compared with

normal subjects, as a result of hepatic insulin insufficiency (Hilding et al., 1995).

Modern insulin management using an insulin pump (continuous subcutaneous insulin infusion, CSII) (Pickup and Keen, 2002) or long-acting insulin analogs such as insulin glargine (Rosenstock et al., 2000) or insulin detemir provides stable and peakless insulin levels, particularly compared with NPH insulin. These modern insulin regimens reduced the risk of hypoglycemic events and, in turn, allow for better glycemic control. In terms of nocturnal glycemic control, some reports have indicated that the dawn phenomenon is decreased with CSII or glargine (Pickup and Renard, 2008).

Here, we investigated the nocturnal fluctuations in glucose, IGFBP-1 and free IGF-1 levels with three basal insulin regimens (CSII, insulin glargine, NPH insulin) that are commonly used by patients with type 1 diabetes in Japan. The aim of this study was to compare the nocturnal IGFBP-1 overproduction and blood glucose fluctuation control in terms of onset of the dawn phenomenon with these insulin regimens.

Research Design and Methods

Subjects

We enrolled 62 Japanese type 1 diabetes mellitus patients from the University of Yamanashi, who were being treated with intensive insulin therapy to achieve near-normal glycemic control while avoiding severe hypoglycemia. Children were enrolled after parental or patient written informed consent was obtained, and adults provided written informed consent. This study was approved by the ethical committee of University of Yamanashi.

Exclusion criteria included diabetes diagnosed within the past 6 months (2 patients), poor glycemic control with HbA1c level >10.0% (5 patients), frequent hypoglycemia (1 patient), acute or chronic illness (1 patient) or ketoacidosis (0 patient). Patients who ate a midnight snack as a result of fear of hypoglycemia were also excluded (5 patients). As a result, 48 patients participated in and completed the study, of which 20 were male and 28 were female. The mean age of the patients was 14.4 years (range 9.9–24.5 years) and the mean time since diagnosis was 6.0 years (0.7–18.8 years). The mean HbA1c level was 7.9% (5.7–9.8%) and the mean body mass index was 21.2 kg/m^2 (15.5–24.9 kg/m^2), and the mean body mass index–standard deviation score (BMI-SDS) was 0.7 (−1.8 to 2.7 SD).

Clinical study design

Patients were classified according to their basal insulin therapy with either NPH (29 patients), glargine (12 patients) or CSII (7 patients) (**Table 1**). The groups were comparable in terms of age, diabetes duration, insulin doses and HbA1c levels (NS between groups), but different in terms of sex. In the NPH group, all patients received multiple daily injection (MDI) with once daily NPH injection at bedtime and preprandial regular insulin (11 patients) or insulin analog (aspart, 8 patients; lispro, 10 patients lispro). In the glargine group, all patients also received MDI with once daily injection of glargine (Lantus®, Sanofi-Aventis, Japan) at bedtime, and their preprandial insulin was insulin analog only (aspart, 5 patients; lispro, 7 patients). In the CSII group, all of the patients were female and were treated with insulin aspart administered by Medtronic Mini Med 505 (2 patients) or NIPRO (5 patients) insulin pumps. Their insulin pumps were set, by the physician, to deliver a constant basal insulin rate during the experimental period. The basal CSII dose was set at 45–60% of the total daily insulin dose and was comparable with the bedtime doses of insulin used in the MDI groups.

Table 1 Baseline characteristics of the patients according to the basal insulin regimen.

	NPH (n=29)	Glargine (n=12)	CSII (n=7)
males/females (n)	13/16	7/5	0/7
age (years)	14.0±0.5	14.9±0.7	15.0±0.6
time since diagnosis (years)	5.6±0.8	7.4±1.4	5.3±1.1
height (cm)	152.1±2.0	154.0±3.4	153.4±0.9
weight (kg)	48.9 ±2.1	53.1±3.6	51.2 ±2.1
body mass index (kg/m^2)	20.8±0.5	22.2±1.0	21.7±0.7
body mass index-standard deviation scores	0.6±0.2	0.9±0.3	0.8±0.3

Data are n or mean ± SEM

There were no differences between groups in terms of any of the baseline characteristics

At the research center, the subjects administered their preprandial insulin injection, including a bolus infusion in the CSII group, and ate dinner at 1800 h, which was calculated by a dietitian to be appropriate for the patient's age in terms of calories. NPH or glargine was administered at 2100 h, and breakfast was at 0800 h. None of the patients in any group ate a bedtime snack. An intravenous catheter filled with physiological saline was inserted and blood samples were obtained every 2 h from 2300 h to 0700 h, without waking the patient up, for measurement of plasma glucose, IGFBP-1 and free IGF-1 levels. The HbA1c, IGF-1 and IGFBP-3 levels were determined at 0700 h. We assessed the nocturnal profiles of these factors and the appearance of the dawn phenomenon in each group.

Definition of dawn phenomenon

Dawn phenomenon was defined as previously described (Kobayashi et al., 1997) as: 1) change in plasma glucose from 0500 h to 0700 h of >20 mg/dl; 2) plasma glucose level at 0700 h of >140 mg/dl; and 3) no antecedent hypoglycemia.

Assays

Blood samples were centrifuged (2000×g, 5 min, 4 °C) rapidly after sampling, and plasma or serum were aliquoted and frozen at −20 °C. The plasma glucose concentration was measured by the glucose electrode method (Glucose Auto and Stat, ARKRAY, Japan). HbA1c was measured by high performance liquid chromatography (Hi Auto H1c, ARKRAY). Serum IGFBP-1 and free IGF-1 concentrations were measured by immunoradiometric assays (Diagnostics Systems Laboratories, Webster, TX, USA). The sensitivity of the IGFBP-1 assay was 2.0 ng/ml. Intraassay imprecision was 6.5% at 7.0 ng/ml and 5.3% at 70.0 ng/ml. The sensitivity of the free IGF-1 assay was 0.4 ng/ml. Intraassay imprecision was 4.9% at 0.02 ng/ml and 7.8% at 2.0 ng/ml, respectively.

Statistical analysis

Clinical results are presented as means ± standard error of the mean. BMI-SDS scores were calculated based on a previous report of BMI standardized centile curves in Japanese children and adolescents (Inokuchi et al., 2006). The distributions of the data were examined for normality using the Kolmogorov-Smir-

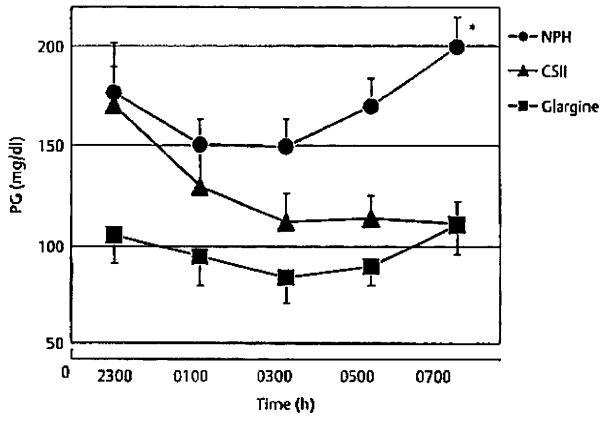

Fig. 1 Nocturnal blood glucose profiles in patients with type 1 diabetes treated with NPH insulin (n=29, black circles), CSII (n=7, black triangles) or insulin glargine (n=12, black squares) based regimens. Data are means±SEM. *p<0.001, blood glucose levels with NPH at 0300h vs. 0700h.

nov goodness of fit test. Log transformation of IGFBP-1 was necessary for statistical testing purpose, but we present non-transformed values for clear comprehension. The Mann-Whitney U test was used to compare the three groups. Cross-correlation was used to determine the association between IGFBP-1 and free IGF-1.

Results

Insulin doses

As shown in **Table 2**, the mean daily dose of insulin was comparable in both groups (although numerically higher in the glargine group), but the proportion of insulin administered as basal insulin was significantly higher in the CSII group than in the NPH or glargine groups.

Nocturnal glycemic profiles

The nocturnal changes in blood glucose levels are shown in ○ **Fig. 1**. At bedtime (2300h), the blood glucose level was 170.0±31.8mg/dl in the CSII group, which was comparable to that in the NPH group (176.5±13.2mg/dl). In the NPH group, the blood glucose level was 149.5±13.6mg/dl at 0300h, which increased significantly to 199.4±15.3mg/dl at 0700h (p<0.001). In the CSII group, the mean glucose level during the morning was stable from at 0300h (112.5±13.6mg/dl) to 0700h (111.2±11.3mg/dl). In the glargine group, there was a mild increase in nocturnal glucose levels between 0300h and 0700h (84.2±13.6mg/dl to 111.2±15.6mg/dl), but the blood glucose level at 2300h was the lowest of all three groups. The dawn phenomenon was significantly more frequent in the NPH group (62.1%) than in the glargine (16.6%, p<0.05) or CSII (14.3%, p<0.05) groups (**Table 2**).

Nocturnal IGFBP-1 and free IGF-1 profiles

Patients in the NPH group were younger than those in the other groups, and the mean total IGF-1 levels were distributed in levels corresponding to the age of the patients in each group (**Table 1**). Nevertheless, the circulating IGFBP-3 levels, the primary IGF-1 carrier protein, were comparable between the three groups.

Table 2 Effects of the three insulin regimens on total IGFBP-1 and IGF-1 levels and dawn phenomenon.

	NPH (n=29)	Glargine (n=12)	CSII (n=7)
basal insulin rate (%)	31.5±1.4	32.3±1.4	54.1±2.7*
daily insulin dose (U/kg)	1.1±0.1	1.3±0.1	1.1±0.1
HbA1c (%)	8.0±0.3	7.8±0.3	8.1±0.5
total IGF-1 (ng/ml)	244.0±19.6	306.2±26.6	351.3±30.2
IGFBP-3 (μg/ml)	4.2±0.1	4.0±0.2	4.2±0.1
Dawn phenomenon (%, n)	62.1 (18/29)	16.6 (2/12)**	14.3 (1/7)**

Data are n or mean±SEM
* p<0.05 vs. NPH and glargine groups
** p<0.05 vs. NPH group

The nocturnal IGFBP-1 and free IGF-1 profiles are shown in ○ **Fig. 2**. The IGFBP-1 levels were inversely correlated with free IGF-1 levels at 0700h in all patients (r=−0.302, p<0.05). In all groups, the IGFBP-1 levels were markedly higher than the reference range (15–50ng/ml) and were particularly higher in the morning. Of note, the IGFBP-1 levels in the NPH group increased by about 10-fold between 2300h and 0700h (from 21.0±3.6ng/ml to 200.3±21.8ng/ml), and the free IGF-1 levels inversely decreased by about half over the same time (from 7.5±1.1ng/ml to 3.3±0.6ng/ml). In the CSII group, the IGFBP-1 levels increased from 19.6±5.0ng/ml to 95.2±17.9ng/ml (p<0.001 vs. NPH) and the free IGF-1 levels were stable (5.7±1.3ng/ml at 2300h and 5.3±1.4ng/ml at 0300h). Glargine partly suppressed the morning rise in IGFBP-1 (25.0±7.2ng/ml at 2300h; 53.1±6.3ng/ml at 0700h; p<0.001 vs. NPH) and the free IGF-1 levels remained stable between 2300h (4.5±0.5ng/ml) and 0700h (4.3±0.7mg/ml).

Discussion

In this study, we investigated the nocturnal fluctuations in glucose, IGFBP-1 and free IGF-1 levels in patients with type 1 diabetes, and compared these profiles between three basal insulin regimens that are commonly used in Japan (CSII, insulin glargine, NPH insulin). We found that the dawn-time glucose rise was significant in patients with NPH, with 60% of patients exhibiting the dawn phenomenon, and the circulating IGFBP-1 levels were markedly increased before breakfast and the free IGF-1 levels were substantially decreased. In the CSII group (the insulin pumps were set to deliver a constant basal insulin rate), the dawn-time glucose levels were stable and the dawn phenomenon was less frequent than in the NPH group. The nocturnal IGFBP-1 levels were also stable with CSII and the morning IGFBP-1 level was lower than those in patients with NPH. In the glargine group, the dawn-time glucose levels were stable and the dawn phenomenon was less frequent than in the NPH group. The nocturnal IGFBP-1 levels exhibited a normal morning rise in the glargine group.

The results of this study should be considered after taking into account limitations of the study. First, this was an open-label, non-randomized, cross sectional study, in which patients continued their prior insulin regimen without optimization of their insulin doses prior to the study. Second, the glucose levels at 2300h were markedly different between the glargine group and the CSII and NPH group. As a result, direct comparison of the

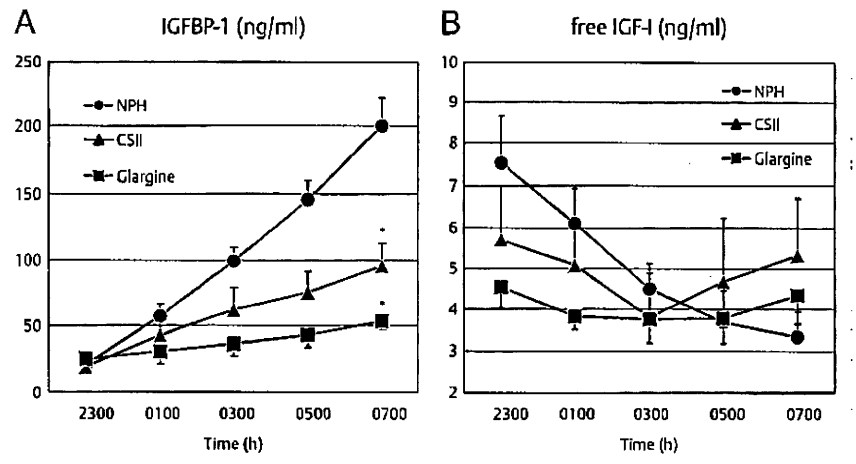

Fig. 2 Nocturnal IGFBP-1 (A) and free IGF-1 (B) profiles in patients treated with NPH insulin (n = 29, black circles), CSII (n = 7, black triangles) or insulin glargine ((n = 12, black squares) based regimens. Data are means ± SEM. *p < 0.05 vs. NPH group at 0700 h.

findings between the glargine group and the CSII and NPH groups should be made with care. This finding was surprising and it is unclear why this occurred, because the total insulin doses, evening meal size and preprandial insulin doses were comparable in all three groups. However, the high glucose level in CSII group may be attributable to significantly higher proportion of basal insulin in the CSII group (54.1%) compared with the NPH (31.5%) and glargine groups (32.4%). Therefore, it is possible that the prandial dose was inadequate in the CSII group, meaning postprandial hyperglycemia was not corrected as quickly as in the glargine group. Alternatively, the basal doses of insulin were not optimally titrated, particularly in the CSII and NPH groups because of the fear of hypoglycemia, for example. In this study, we could not differentiate between the waning of the insulin effect and the effect of insulin resistance on dawn phenomenon, because we could not assess the exact timing of the GH surge because blood samples were taken every 2 h. A future study in which blood samples are taken more frequently, perhaps every 5–10 min, would allow accurate identification of the timing of the GH surge and its associated effect on IGF-1, IGFBP-1 and glucose levels. In addition, we could not measure the nocturnal free insulin profile, because assays for insulin analogs (insulin aspart, lispro or glargine) are often inaccurate because of limited cross-reactivity for each analog. Despite these limitations, we believe that this study provides valuable information regarding the effect of insulin regimens on the dawn phenomenon. These findings need to be further investigated in a randomized, controlled cross-over study design, with titration of insulin doses in advance of the study day to limit the influence of sub-optimal glycemic control and blood samples should be obtained more frequently to identify the GH surge.

The main cause of dawn phenomenon is considered to be the waning of insulin action, particularly in NPH insulin-based MDI regimens, in which the insulin doses are often lower than recommended to prevent unwanted hypoglycemia. The second cause of the dawn phenomenon is insulin resistance, which is mediated by increased GH surges. The morning surge in IGFBP-1 levels, which binds to IGF-1, may also play a role in the dawn phenomenon. A study by Frystyk et al. showed that the highest IGFBP-1 levels (15–50 ng/ml) in healthy children are observed before breakfast (Frystyk et al., 2003), but the IGFBP-1 levels in our patients with type 1 diabetes were in the range 50–300 ng/ml at the same time, particularly in the NPH group. In children and adolescents with poorly controlled type 1 diabetes, circulating total IGF-1 levels are often inappropriately low compared with the high GH levels, possibly derived from an acquired state of hepatic GH resistance (Dunger et al., 2005). Therefore, normalization of the GH-IGF-1 axis is essential for prevention of poor glycemic control.

Insulin pump therapy and insulin glargine could maintain stable insulin levels compared with NPH. Of note, the dose of NPH insulin used in this study was not sufficient to maintain the required level of insulin until breakfast, whereas both insulin glargine and CSII maintains insulin at the appropriate level and were able to suppress IGFBP-1 release. It is of interest to determine the effect of insulin detemir on nocturnal IGFBP-1 and IGF-1 levels and the dawn phenomenon, particularly because insulin detemir can be used either once daily or twice daily as part of an MDI regimen. Understanding the effect of detemir dosing on the dawn phenomenon will be of value to help clinicians and patients to use insulin detemir in the best possible way for the patient (Le Floch et al., 2009).

We conclude that the dawn phenomenon is induced by the waning of insulin effect during the early morning before breakfast and was prevented in this study by CSII and glargine therapy. A decrease in free IGF-1, due to binding with IGFBP-1, leads to a loss of its metabolic effect and may affect insulin resistance in the morning. Insulinopenia affects the IGFBP-1 level; thus, a stable basal insulin level should be maintained, irrespective of the regimen used. Modern insulin regimens based on CSII or basal insulin analogs, which offer profiles without marked peaks in activity and with protracted duration of action provide all-night insulin availability with a lower risk of hypoglycemia compared with NPH insulin. Appropriate insulin therapy to maintain stable insulin levels overnight and in the morning will allow better glycemic control and prevent the dawn phenomenon. Patients who regularly experience the dawn phenomenon should consider either changing their insulin dose, or switching to an alternative insulin regimen that provides more stable insulin levels to minimize the impact of the dawn phenomenon on their overall glycemic control.

Acknowledgements

We would like to thank all of the staff and participants involved in this study. This study was not supported by any research grants from any pharmaceutical company and the authors have no conflicts of interest to declare.

Conflict of interest: None.

References

1 *Dunger DB, Regan FM, Acerini CL.* Childhood and adolescent diabetes. Endocr Dev 2005; 9: 107–120
2 *Frystyk J, Nyholm B, Skjaerbaek C et al.* The circulating IGF system and its relationship with 24 h glucose regulation and insulin sensitivity in healthy subjects. Clin Endocrinol 2003; 58: 777–784
3 *Hilding A, Brismar K, Degerblad M et al.* Altered relation between circulating levels of insulin-like growth factor-binding protein-1 and insulin in growth hormone-deficient patients and insulin-dependent diabetic patients compared to that in healthy subjects. J Clin Endocrinol Metab 1995; 80: 2646–2652
4 *Kobayashi K, Amemiya S, Sawanobori E et al.* Role of IGF binding protein-1 in the dawn phenomenon and glycemic control in children and adolescents with IDDM. Diabetes Care 1997; 20: 1442–1447
5 *Lang CH, Vary TC, Frost RA.* Acute in vivo elevation of insulin-like growth factor (IGF) binding protein-1 decreases plasma free IGF-I and muscle protein synthesis. Endocrinology 2003; 144: 3922–3933
6 *Inokuchi M, Hasegawa T, Anzo M et al.* Standardized centile curves of body mass index for Japanese children and adolescents based on the 1978–1981 national survey data. Ann Hum Biol 2006; 33: 444–453
7 *Le Floch JP, Lévy M, Mosnier-Pudar H et al.* Assessment of Detemir Administration in Progressive Treat-to-Target Trial (ADAPT) Study Group. Comparison of once- versus twice-daily administration of insulin detemir, used with mealtime insulin aspart, in basal-bolus therapy for type 1 diabetes: assessment of detemir administration in a progressive treat-to-target trial (ADAPT). Diabetes Care 2009; 32: 32–37
8 *Lee PD, Giudice LC, Conover CA et al.* Insulin-like growth factor binding protein-1: Recent findings and new directions. Proc Soc Exp Biol Med 1997; 216: 319–357
9 *Perriello G, De Feo P, Torlone E et al.* Nocturnal spikes of growth hormone secretion cause the dawn phenomenon in type 1 (insulin-dependent) diabetes mellitus by decreasing hepatic (and extrahepatic) sensitivity to insulin in the absence of insulin waning. Diabetologia 1990; 33: 52–59
10 *Pickup J, Keen H.* Continuous subcutaneous insulin infusion at 25 years: Evidence base for the expanding use of insulin pump therapy in type 1 diabetes. Diabetes Care 2002; 25: 593–598
11 *Pickup JC, Renard E.* Long-acting insulin analogs versus insulin pump therapy for the treatment of type 1 and type 2 diabetes. Diabetes Care 2008; 31 (Suppl 2): S140–S145
12 *Rosenstock J, Park G, Zimmerman J, U. S. Insulin Glargine (HOE 901) Type 1 Diabetes Investigator Group.* Basal insulin glargine (HOE 901) versus NPH insulin in patients with type 1 diabetes on multiple daily insulin regimens. U. S. Insulin Glargine (HOE 901) Type 1 Diabetes Investigator Group. Diabetes Care 2000; 23: 1137–1142
13 *Schmidt MI, Hadji-Georgopoulos A, Rendell M et al.* The dawn phenomenon, an early morning glucose rise: implications for diabetic intraday blood glucose variation. Diabetes Care 1981; 4: 579–585
14 *van Cauter E, Desir D, Decoster C et al.* Nocturnal decrease in glucose tolerance during constant glucose infusion. J Clin Endocrinol Metab 1989; 69: 604–611

THE JOURNAL OF BIOLOGICAL CHEMISTRY VOL. 285, NO. 48, pp. 37884–37894, November 26, 2010

Regulation of Ghrelin Signaling by a Leptin-induced Gene, Negative Regulatory Element-binding Protein, in the Hypothalamic Neurons*[S]

Received for publication, May 27, 2010, and in revised form, September 17, 2010 Published, JBC Papers in Press, September 28, 2010, DOI 10.1074/jbc.M110.148973

Tadasuke Komori[‡], Asako Doi[§], Hiroto Furuta[§], Hiroshi Wakao[¶], Naoyuki Nakao[‖], Masamitsu Nakazato[**], Kishio Nanjo[§], Emiko Senba[‡], and Yoshihiro Morikawa[‡1]

From the [‡]Department of Anatomy and Neurobiology, the [§]First Department of Medicine, and [‖]Department of Neurological Surgery, Wakayama Medical University, 811-1 Kimiidera, Wakayama 641-8509, Japan, the [¶]Department of Environmental Biology, School of Medicine, Hokkaido University, N15W7, Sapporo 060-8638, Japan, and the [**]Division of Neurology, Respirology, Endocrinology, and Metabolism, Department of Internal Medicine, Miyazaki Medical College, University of Miyazaki, Kihara, Kiyotake, Miyazaki 889-1692, Japan

Leptin, the product of the *ob* gene, plays important roles in the regulation of food intake and body weight through its receptor in the hypothalamus. To identify novel transcripts induced by leptin, we performed cDNA subtraction based on selective suppression of the polymerase chain reaction by using mRNA prepared from the forebrain of leptin-injected *ob/ob* mice. One of the genes isolated was a mouse homolog of human negative regulatory element-binding protein (NREBP). Its expression was markedly increased by leptin in the growth hormone secretagogue-receptor (GHS-R)-positive neurons of the arcuate nucleus and ventromedial hypothalamic nucleus. The promoter region of GHS-R contains one NREBP binding sequence, suggesting that NREBP regulates GHS-R transcription. Luciferase reporter assays showed that NREBP repressed GHS-R promoter activity in a hypothalamic neuronal cell line, GT1-7, and its repressive activity was abolished by the replacement of negative regulatory element in GHS-R promoter. Overexpression of NREBP reduced the protein expression of endogenous GHS-R without affecting the expression of ob-Rb in GT1-7 cells. To determine the functional importance of NREBP in the hypothalamus, we assessed the effects of NREBP on ghrelin action. Although phosphorylation of AMP-activated protein kinase α (AMPKα) was induced by ghrelin in GT1-7 cells, NREBP repressed ghrelin-induced AMPKα phosphorylation. These results suggest that leptin-induced NREBP is an important regulator of GHS-R expression in the hypothalamus and provides a novel molecular link between leptin and ghrelin signaling.

Obesity develops when food intake exceeds compensatory increases in energy expenditure, and energy is accumulated as fat (1). Food intake is controlled by the precise coordination between the neural circuitry and peripheral factors that derive from fat, gut, and pancreas. The peripheral factors transduce their signals by binding to the receptors in the hypothalamus and regulate production of the orexigenic and the anorexigenic peptides in the specific subsets of hypothalamic neurons (2). Thus, the hypothalamus is critical in integrating signals from the peripheral factors in the neural circuitry.

Leptin, an adipocyte-derived hormone (3), is a key negative regulator of food intake and energy expenditure. Circulating leptin enters the brain through the blood-brain barrier (4) and exerts its effects through binding to the long form of the leptin receptor ob-Rb (5) expressed in the hypothalamus, including the arcuate nucleus, ventromedial hypothalamic nucleus (VMH),[2] dorsomedial hypothalamic nucleus, lateral hypothalamic nucleus, and paraventricular hypothalamic nucleus (6). For example, in the hypothalamic arcuate nucleus, leptin suppresses food intake via decreased expression of the orexigenic peptides, neuropeptide Y, and agouti-related peptide and increased expression of the anorexigenic peptides, proopiomelanocortin, and cocaine- and amphetamine-regulated transcript (6–9).

Although the administration of leptin reverses obesity caused by its deficiency in mice and humans (10, 11), obesity caused by total deficiency of leptin is uncommon in humans. Instead, most obese humans are characterized by resistance to leptin. Some mechanisms are thought to be involved in the development of leptin resistance: circulating factors that bind to leptin and inhibit its physiological functions, such as C-reactive protein and the soluble form of the leptin receptor (12, 13), defects in the transport of leptin across the blood-brain barrier, and impairments of the intracellular signaling cascade from leptin receptor.

In the hypothalamus, binding of leptin to ob-Rb can mediate transcription of target genes mainly via the activation of the JAK2 signal transducer and activator of transcription 3 pathway

* This work was supported by Grant-in-aid for Scientific Research 17019047 on Priority Areas "Applied Genomics" from the Ministry of Education, Culture, Sports, Science and Technology of Japan. This work was also supported by Grant-in-aid for Scientific Research 13204074 on Priority Areas "Medical Genome Science" from the Ministry of Education, Culture, Sports, Science and Technology of Japan; a grant provided by the Ichiro Kanehara Foundation; and a research grant on Priority Areas from Wakayama Medical University.

The nucleotide sequence(s) reported in this paper has been submitted to the DDBJ/GenBank™/EBI Data Bank with accession number(s) AB546195.

[S] The on-line version of this article (available at http://www.jbc.org) contains supplemental Figs. S1 and S2.

[1] To whom correspondence should be addressed: Dept. of Anatomy and Neurobiology, Wakayama Medical University, 811-1 Kimiidera, Wakayama 641-8509, Japan. Tel. and Fax: 81-73-441-0617; E-mail: yoshim@wakayama-med.ac.jp.

[2] The abbreviations used are: VMH, ventromedial hypothalamic nucleus; AMPK, AMP-activated protein kinase; GHS-R, growth hormone secretagogue-receptor; NREBP, negative regulatory element-binding protein.

(14). Among them, SOCS3 (suppressor of cytokine signaling 3) negatively regulates hypothalamic leptin signaling via the suppression of JAK2 activation and contributes to the development of a leptin-resistant state (15). Previously, White *et al.* (2000) have identified four novel leptin-induced transcripts (LRG-47, T cell-specific guanine nucleotide triphosphate-binding protein, RC10-11, and Stra-13) from a hypothalamic neuronal cell line, GT1-7, stimulated with leptin (16). However, the roles of leptin-induced molecules in feeding behavior and energy metabolism remain unknown except for neuropeptides and SOCS3. Therefore, the identification of leptin-induced transcripts is of substantial biomedical importance. In the present study, we identified a mouse homolog of human negative regulatory element-binding protein (NREBP), a transcriptional repressor, as a leptin-induced transcript, which repressed the expression of growth hormone secretagogue-receptor (GHS-R) in the hypothalamus.

EXPERIMENTAL PROCEDURES

Animals—Male C57BL/6J lean and *ob/ob* mice (8 to 10 weeks old) were obtained from our breeding colony using heterozygous (*ob*/+) breeding pairs. Mice were housed in specific pathogen-free facilities, in light (12 h light/dark cycle), temperature (22–25 °C), and humidity (50–60% relative humidity) controlled conditions. Mice were fed a standard diet (MF; Oriental Yeast, Tokyo, Japan) and water *ad libitum*. At all times, the experiments were performed under the control of the Animal Research Control Committee in accordance with the Guidelines for Animal Experiments of Wakayama Medical University and Japanese Government Notification on Feeding and Safekeeping of Animals (No. 6) and the National Institutes of Health Guide for the Care and Use of Laboratory Animals. Every effort was made to minimize the number of animals used and their suffering.

Injection of Leptin in ob/ob Mice—Mice who had fasted for 9 h (starting from 9:00 a.m.) were injected intravenously with PBS, pH 7.4, or recombinant mouse leptin (R&D Systems, Minneapolis, MN) dissolved with PBS at a dose of 10 μg/g body weight.

Cloning of Leptin-induced Sequences—Total RNAs from the forebrain of *ob/ob* mice 1 h after the intravenous injection of PBS or mouse leptin were prepared using TRI reagent (Molecular Research Center, Cincinnati, OH) as described previously (17). Isolated mRNA from 200 μg of total RNA was obtained with a FastTrack 2.0 mRNA isolation kit (Invitrogen). To select leptin-induced transcripts in the forebrain, cDNA subtraction based on selective suppression of PCR was performed with PCR-Select cDNA subtraction kit (Clontech, Palo Alto, CA) following the manufacturer's protocol. Double-stranded cDNAs were synthesized from 2 μg of mRNAs using avian myeloblastosis virus reverse transcriptase and T4 DNA polymerase. cDNAs derived from *ob/ob* mice injected with leptin (tester pool) and cDNAs from *ob/ob* mice injected with PBS (driver pool) were digested with the restriction enzyme RsaI. Two types of adapter, provided by the manufacturer, were independently ligated to the tester cDNAs. Each of the tester cDNA pools was hybridized with excess from the driver cDNA pool and incubated at 68 °C for 9 h (first hybridization). Then, the two samples from the first hybridization was immediately mixed (second hybridization), and the resulting annealed material was amplified by suppression PCR: 27 cycles of 94 °C for 30 s, 66 °C for 30 s, and 72 °C for 1.5 min. The amplified PCR products were subtractive, which presented the differentially expressed genes in the tester population compared with the driver population, and were ligated into the T/A cloning vector pCRII (Invitrogen). The individual cDNA inserts were sequenced using T7 primer by an automated sequencer (ABI PRISM 310 Genetic Analyzer, PerkinElmer Life Sciences). Sequence homology searches were done using the Basic Local Alignment Tool program against the National Center for Biotechnology Informatics database, which includes entries from GenBank™, the European Molecular Biology Laboratory, and DNA Database of Japan databases. To verify the selective expression in the brain of *ob/ob* mice injected with leptin, we analyzed differential expression of the individual cDNA sequences on Northern blots with total RNA from forebrains of PBS- and leptin-injected *ob/ob* mice.

Cell Culture—The mouse hypothalamic neuronal cell line, GT1-7 (18), a gift from Dr. Pamela L. Mellon (University of California, La Jolla, CA), was grown in DMEM with 10% fetal calf serum, 100 units/ml of penicillin, and 100 μg/ml of streptomycin (all from Invitrogen). Cells were grown at 37 °C in a humidified atmosphere of 5% CO_2 and 95% air.

Preparation of Probes for NREBP—In the present study, we prepared two types of fragments of NREBP: a 290-bp EcoRI-SalI cDNA fragment of NREBP (coding region 1–275) and a 654-bp EcoRI-NotI cDNA fragment of NREBP (coding region 4492–5110). These fragments were ligated into pBluescript SK(+) vector (Invitrogen) and linearized by cutting with appropriate restriction enzymes.

The probe for Northern blot analysis was prepared by using Megaprime DNA labeling systems and [^{32}P]dCTP (both from Amersham Biosciences). The radioisotope-labeled probes for *in situ* hybridization histochemistry were prepared by using appropriate RNA polymerases (T7 RNA polymerase for the antisense probe and T3 RNA polymerase for the sense probe) and [^{35}S]dUTP (PerkinElmer Life Sciences). We used two types of probes (coding region 1–275 and 4492–5110) for Northern blot analysis and a radioisotope-labeled probe for *in situ* hybridization histochemistry. Similar results were obtained with both probes. We thus reported results with the probe prepared by using the fragment of the NREBP (coding region 1–275).

Northern Blot Analysis—Northern blot analysis was performed with some modifications as described previously (17). Briefly, at 1 h after PBS or leptin injection, *ob/ob* mice were deeply anesthetized with diethyl ether, and the brains were quickly removed. Total RNA was isolated from mediobasal hypothalami (defined caudally by the mammillary bodies, rostrally by the optic chiasm, laterally by the optic tract, and superiorly by the apex of the hypothalamic third ventricle) by using TRI Reagent. After separation on 1.2% agarose gels containing 2.4% formaldehyde, total RNA was transferred to positively charged nylon membranes (Roche Diagnostics). For the tissue blot analysis, mouse Multiple Tissue Northern blot was obtained from Clontech Laboratories. Then, the membranes were hybridized with the ^{32}P-labeled NREBP probe in a quick hybridization solution (Stratagene, La Jolla, CA) at 68 °C for 2 h.

After washing twice in 2× SSC buffer (1× SSC = 44.6 μmol/l sodium chloride, 5 μmol/l trisodium citrate, pH 7.0) containing 0.1% SDS at 68 °C for 15 min, and once in 0.1× SSC buffer containing 0.1% SDS at 68 °C for 20 min, the membranes were exposed to x-ray films for an appropriate period. The membranes were stripped and rehybridized with probe for 18 S ribosomal RNA or GAPDH.

In Situ Hybridization Histochemistry—In situ hybridization histochemistry using radioisotope-labeled probes was carried out as described previously (19). Briefly, at 1 h after PBS or leptin injection, *ob/ob* mice were deeply anesthetized with diethyl ether and transcardially perfused with ice-cold 4% paraformaldehyde in PBS. The brains were quickly dissected and postfixed in the same fixative at 4 °C for 16 h. Then, the brains were immersed in 30% sucrose in PBS, embedded in Optimal Cutting Temperature compound (Sakura Finetek, Torrance, CA), and frozen rapidly in cold *n*-hexane on dry ice. Frozen sections were cut on a cryostat (6-μm thickness) and stored at −80 °C.

After treatment with proteinase K (Roche Diagnostics), the sections were postfixed in 4% paraformaldehyde, treated with acetic anhydride, and dehydrated with ethanol. The sections were then hybridized with a sense or antisense ^{35}S-labeled NREBP riboprobe at 55 °C for 16 h. After rinsing in 2× SSC buffer containing 10 mM dithiothreitol, the sections were treated with ribonuclease A (10 μg/ml; Wako Pure Chemical Industries, Tokyo, Japan) at 37 °C for 30 min. The high stringency washes were performed in 0.1× SSC buffer at 55 °C for 15 min. After dehydration with ethanol, the sections were submerged in emulsion (NTB-2; Kodak, Rochester, NY), exposed for the appropriate number of days, and developed in D-19 developer (Kodak). The sections were counterstained with Mayer's hematoxylin through the emulsion and examined under dark field lateral illumination microscopy (XF-WFL, Nikon, Tokyo, Japan). The sense cRNA probe failed to hybridize in the brain (data not shown).

To evaluate the expression of NREBP mRNA in the hypothalamus, every fifth section was picked from a series of consecutive hypothalamic sections (6 μm), and three sections per mouse were counted for the arcuate nucleus, VMH, dorsomedial hypothalamic nucleus, lateral hypothalamic nucleus, and paraventricular hypothalamic nucleus. For each section, cells in the hypothalamus were considered positive for NREBP gene expression if five or more silver grains were found overlying the cell bodies.

In Situ Hybridization Histochemistry Combined with Immunohistochemistry—In situ hybridization histochemistry combined with immunohistochemistry was performed with some modifications as described previously (20). Briefly, the sections were hybridized with an NREBP riboprobe, followed by incubation with 5% normal donkey serum (Jackson ImmunoResearch Laboratories, West Grove, PA). Then, the sections were incubated with goat anti-GHS-R antibody (diluted at 1:200, catalog no. sc-10362, Santa Cruz Biotechnology, Santa Cruz, CA) at 4 °C for 16 h. After washing, they were incubated with biotinylated donkey anti-goat IgG antibody (diluted at 1:400, Jackson ImmunoResearch Laboratories), followed by incubation with HRP-conjugated streptavidin (DAKO, Carpinteria, CA). The peroxidase reaction product was visualized with 0.05% diaminobenzidine tetrahydrochloride (Sigma) and 0.01% H_2O_2. After the reaction, the sections were submerged in the emulsion and counterstained with Mayer's hematoxylin through the emulsion. The specificity of goat anti-GHS-R antibody for immunohistochemistry was confirmed by using the brain sections of GHS-R$^{-/-}$ mice (supplemental Fig. S1, *A* and *B*).

To evaluate the colocalization of NREBP mRNA and GHS-R in the hypothalamus, every fifth section was picked from a series of consecutive hypothalamic sections (6 μm), and three sections per mouse were counted for the arcuate nucleus and VMH. For each section, cells in the arcuate nucleus and VMH were considered positive for NREBP gene expression if five or more silver grains were found overlying the cell bodies and were considered positive for the protein expression of GHS-R if the cell bodies were stained brown.

Plasmid—A fragment of the promoter region of the GHS-R gene (−734 to −121) in pGL3-Basic vector (21) was provided by Dr. Hidesuke Kaji (Kobe University School of Medicine, Kobe, Japan). Full-length mouse NREBP cDNA was obtained by screening a mouse brain cDNA library (Invitrogen) using a standard technique and was ligated into pCMV-SPORT2 vector (Invitrogen).

In Vitro Mutagenesis—In vitro mutagenesis was performed with some modifications as described previously (22). The NRE replacement mutant in the GHS-R promoter was made with a QuikChange site-directed mutagenesis kit (Stratagene). The template DNA (wild-type GHS-R promoter in pGL3-Basic vector) was amplified by using the complementary primer pairs: 5′-GAAGCGGGAGCGTGAGTTTTTTTTTCCGAAGCCCTGGGC-3′ and 5′-GCCCAGGGCTTCGGAAAAAAAAAACTCACGCTCCCGCTTC-3′ (the sites of the nucleotide changes are in boldface type). The PCR amplification protocol was 95 °C for 2 min and then 12 cycles of 95 °C for 30 s, 64 °C for 1 min, 68 °C for 7 min, and a final 10 min extension at 68 °C. To select the mutation-containing synthesized DNA, the PCR product was treated with DpnI endonuclease, which specifically digests the parental DNA template. The product was then self-ligated by using a DNA ligation kit (version 2.1, Takara Bio, Inc., Tokyo, Japan) at 16 °C for 30 min, followed by the transformation into DH-5α competent cells (Invitrogen). The sequences of the mutated regions in GHS-R promoter were confirmed by using the primer pairs RVprimer3 and GLprimer2 (Promega, Madison, WI), both designed for use with pGL3-Basic vector.

Transient Transfection—Transient transfection was carried out with some modifications as described previously (23). Briefly, GT1-7 cells were plated in 24-well plates at a density of 6 × 10^4 cells/well for the luciferase assays or plated in six-well plates at a density of 3 × 10^5 cells/well for Western blot analysis. After incubation in the standard medium for 1 day, the cells were transfected with plasmids of mock or NREBP at indicated concentrations using FuGENE 6 transfection reagent (Roche Diagnostics). For luciferase assays, all transient transfections also included 0.5 μg of the wild type or mutant GHS-R promoter in pGL3-Basic vector and 0.1 μg of *Renilla* luciferase control reporter plasmid (pRL-TK; Promega). All

A

```
1 MAADIEQVFRSFVVSKFREIQQELSSGRSEGQLNGETNPPIEGNQAGDTAASARSLPNEEIVQKIEEVLSGVLDTELRYKPDLKEASRKSRCVSVQTDPT 100
101 DEVPTKKSKKHKKHKNKKKKKKKEKEKKYKRQPEESESKLKSHHDGNLESDSFLKFDSEPSAAALEHPVRAFGLSEASETALVLEPPVVSMEVQESHVLE 200
                K-rich
201 TLKPATKAAELSVVSTSVISEQSEQPMPGMLEPSMTKILDSFTAAPVPMSTAALKSPEPVVTMSVEYQKSVLKSLETMPPETSKTTLVELPIAKVVEPSE 300
301 TLTIVSETPTEVHPEPSPSTMDFPESSITDVQRLPEQPVEAPSEIADSSMTRPQESLELPKTTAVELQESTVASALELPGPPATSILELQGPPVTPVPEL 400
401 PGPSATPVPELSGPLSTPVPELPGPPATVVPELPGPSVTPVPQLSQELPGPPAPSMGLEPPQEVPEPPVMAQELSGVPAVSAAIELTGQPAVTVAMELTE 500
                son-c repeat
501 QPVTTTEFEQPVAMTTVEHPGHPEVTTATGLLGQPEAAMVLELPGQPVATTALELSGQPSVTGVPELSGLPSATRALELSGQSVATGALELPGQLMATGA 600
601 LEFSGQSGAAGALELLGQPLATGVLELPGQPGAPELPGQPVATVALEISVQSVVTTSELSTMTVSQSLEVPSTTALESYNTVAQELPTTLVGETSVTVGV 700
701 DPLMAQESHMLASNTMETHMLASNTMDSQMLASNTMDSQMLASNTMDSQMLASSTMDSQMLASSTMDSQMLATSTMDSQMLATSSMDSQMLATSSMDSQM 800
                son-b repeat
801 LATSSMDSQMLATSSMESQMLASGAMDSQMLASGTMDAQMLASGTMDAQMLASSTQDSAMMGSKSEDPYRLAQDPYRLAQDPYRLGHDPYRLGHDAYRLG 900
901 QDPYRLGHDPYRLTPDPYRVSPRPYRIAPRSYRIAPRPYRLAPRPLMLASRRSMMMSYAAERSMMSSYERSMMSYERSMMSPMAERSMMSAYERSMMSAY 1000
1001 ERSMMSPMAERSMMSAYERSMMSAYERSMMSPMADRSMMSMGADRSMMSSYSAADRSMMSSYSAADRSMMSSYTDRSMMSMAADSYTDSYTDSYTEAYMV 1100
                son-a repeat
1101 PPLPPEEPPTMPPLPPEEPPMTPPLPPEEPPEGPALSTEQSALTADNIWSTEVTLSTGESLSQPEPPVSQSEISEPMAVPANYSMSESETSMLASEAVMT 1200
                P-rich
1201 VPEPAREPESSVTSAPVESAVVAEHEMVPERPMTYMVSETTMSVEPAVLTSEASVISETSETYDSMRPSGHAISEVTMSLLEPAVTISQPAENSLELPSM 1300
1301 TVPAPSTMITTESPVVAVTEIPPVAVPEPPIMAVPELPTMAVVKTPAVAVPEPLVAAPEPPTMATPELCSLSVSEPPVAVSELPALADPEHAITAVSGVS 1400
1401 SLEPSVPILEPAVSVLQPVMIVSEPSVPVQEPTVAVSEPAVIVSEHTQITSPEMAVESSPVIVDSSVMSSQIMKGMNLLGGDENLGPEVGMQETLLHPGE 1500
1501 EPRDGGHLKSDLYENEYDRNADLTVNSHLIVKDAEHNTVCATTVGPVGEASEEKILPISETKEITELATCAAVSEADIGRSLSSQLALELDTVGTSKGFE 1600
                clone 1-42
1601 FVTASALISESKYDVEVSVTTQDTEHDMVISTSPSGGSEADIEGPLPAKDIHLDLPSTNFVCKDVEDSLPIKESAQAVAVALSPKESSEDTEVPLPNKEI 1700
1701 VPESGYSASIDEINEADLVRPLLPKDMERLTSLRAGIEGPLLASEVERDKSAASPVVISIPERASESSSEEKDDYEIFVKVKDTHEKSKKNKNRDKGEKE 1800
1801 KKRDSSLRSRSKRSKSSEHKSRKRTSESRSRARKRSSKSKSHRSQTRSRSRSRRRRRSSRSRSKSRGRRSVSKEKRKRSPKHRSKSRERKRKRSSSRDNR 1900
                SR domain
1901 KAARARSRTPSRRSRSHTPSRRRRSRSVGRRRSFSISPSRRSRTPSRRSRTPSRRSRTPSRRSRTPSRRRRSRSAVRRRSFSISPVRLRRSRT 2000
2001 PLRRRFSRSPIRRKRSRSSERGRSPKRLTDLDKAQLLEIAKANAAAMCAKAGVPLPPNLKPAPPPTIEEKVAKKSGGATIEELTEKCKQIAQSKEDDDVI 2100
2101 VNKPHVSDEEEEEPPFYHHPFKLSEPKPIFFNLNIAAAKPTPPKSQVTLTKEFPVSSGSQHRKKEADSVYGEWVPVEKNGEESKDDDNVFSSSLPSEGRV 2200
2201 KRQGRVKRQMKQPAASHLTVTRCNSLCGTKPQSEKHRIAEKSVITSLPNIGPSMHLWEGSPRYNYLASRFASRLYSSRFWW
```

B

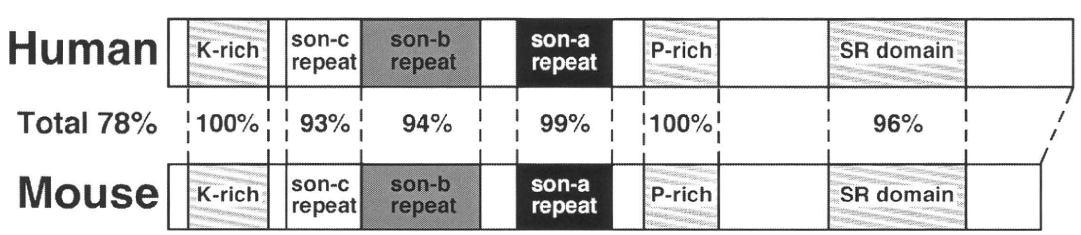

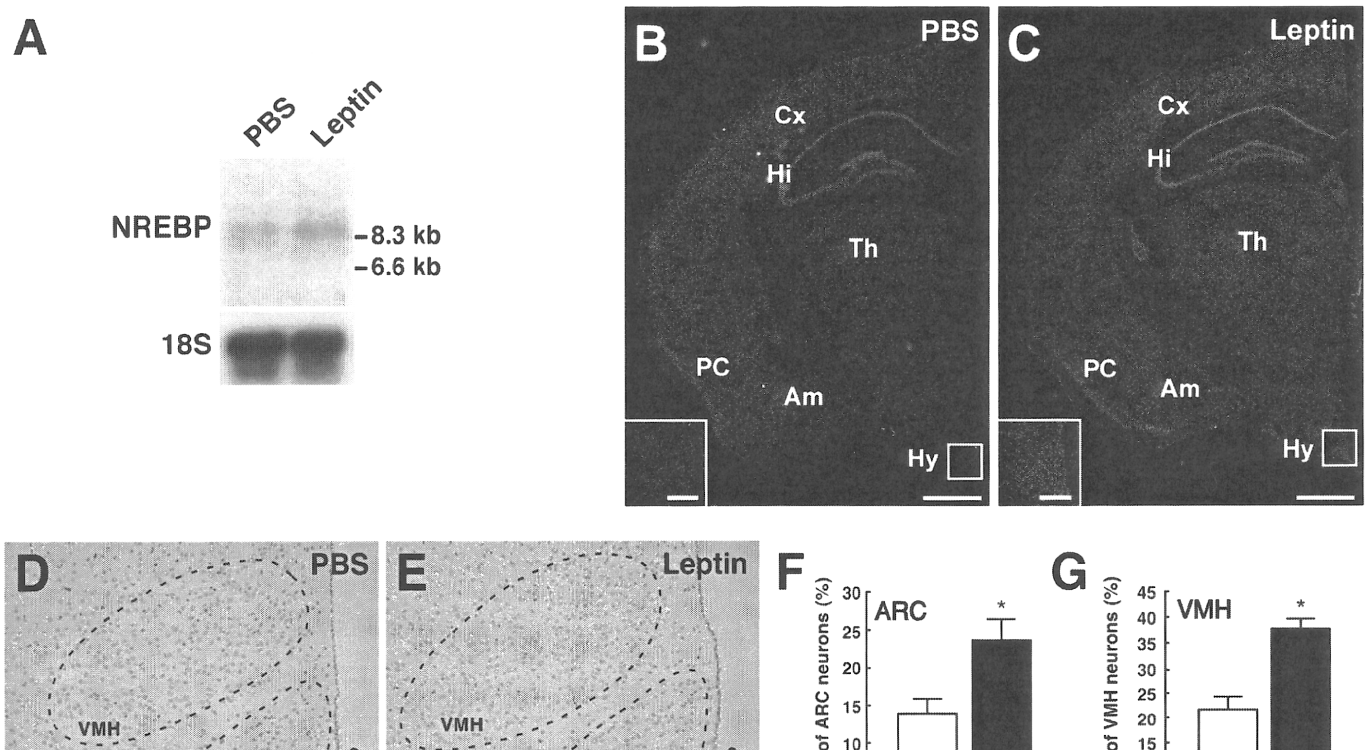

FIGURE 2. **Expression of NREBP in the hypothalamus of PBS- or leptin-injected *ob/ob* mice.** *A*, Northern blot analysis of NREBP mRNA in the hypothalamus of PBS- or leptin-injected *ob/ob* mice. Two micrograms of total RNA isolated from the hypothalamus were separated on agarose gels and then transferred to nylon membranes. The membranes were hybridized with ^{32}P-labeled NREBP probe. The membranes were stripped and rehybridized with probe for 18 S ribosomal RNA to control for loading of the lanes. RNA size markers (in kilobase pairs) are shown to the *right*. *B* and *C*, dark field views of *in situ* hybridization histochemistry for NREBP in the brain of PBS- (*B*) or leptin-injected (*C*) *ob/ob* mice ($n = 4$ per group). The sections were hybridized with ^{35}S-labeled NREBP probe. The *boxed regions* indicated in *B* and *C* are shown at a higher magnification in each inset. *Cx*, cortex; *Hi*, hippocampus; *Th*, thalamus; *PC*, piriform cortex; *Am*, amygdala; *Hy*, hypothalamus. *Scale bars*, 1 mm; 200 μm in *insets*. *D* and *E*, semi-bright field views of *in situ* hybridization histochemistry for NREBP in the hypothalamus of PBS- (*D*) or leptin-injected (*E*) *ob/ob* mice ($n = 4$ per group). The arcuate nucleus and VMH are shown by the *dotted lines*. *ARC*, arcuate nucleus; *3v*, third ventricle. *Scale bars*, 200 μm. *F* and *G*, NREBP-expressing cells in PBS- (*white bar*) or leptin-injected (*black bar*) *ob/ob* mice were quantified as the percentage of positive neurons in the total neurons of the arcuate nucleus (*F*) and VMH (*G*). Data represent the means ± S.E. *, $p < 0.05$ Student's *t* test.

cells were transfected with FuGENE 6 transfection reagent (μl) and DNA (μg) at a ratio of 3:1.

Luciferase Assay—Luciferase assay was performed by using a Dual-Luciferase reporter assay system according to the manufacturer's instructions (Promega) with some modifications as described previously (22). Briefly, at 48 h after the transfection, the cells were washed twice with PBS and lysed by passive lysis buffer (Promega). The luciferase activities were defined as the ratio of *Photinus pyralis* luciferase activity from pGL3-Basic derivatives relative to *Renilla reniformis* luciferase activity from pRL-TK, which reflected the efficiency of transfection.

Treatment of Ghrelin in Mock- or NREBP-transfected GT1-7 Cells—At 3 days after the transfection of mock or NREBP, GT1-7 cells were treated with saline or ghrelin (Peptide Institute, Osaka, Japan) dissolved with saline at a dose of 100 nM. Five min after treatment, the cells were used as samples for Western blot analysis.

Western Blot Analysis—Western blot analysis was performed with some modifications as described previously (20). Briefly, at 3 h after PBS or leptin injection, *ob/ob* mice were deeply anesthetized with diethyl ether, and the brains were quickly removed. Lysates from the cultured cells or the mediobasal hypothalami were prepared by using RIPA buffer (Upstate Biotechnology, Lake Placid, NY) containing protease inhibitor mixture (Upstate Biotechnology), 1 mM orthovanadate, 1 mM sodium fluoride, and 1 mM phenylmethylsulfonyl fluoride. The protein concentrations in the lysates were determined by using a BCA protein assay kit (Pierce, Rockford, IL). Ten micrograms of protein from cultured cells or 20 μg of protein from the tissues were separated by SDS-PAGE and transferred to nitrocellulose membranes (GE Healthcare). After blocking with 5% ECL blocking reagent (GE Healthcare) at room temperature for 1 h, the blotted membranes were incubated with rabbit anti-GHS-R antibody (diluted at 1:500, cata-

FIGURE 1. **The structure of mouse NREBP.** *A*, amino acid sequence of mouse NREBP. The *white box*, *shaded box*, and *black box* indicate son-c, son-b, and son-a repeats, respectively. The Lys-rich, Pro-rich, and SR domain are *underlined*. The region that came from cDNA subtraction is *underlined twice* (clone 1-42). *B*, schematic representation of homology between human NREBP and mouse NREBP. The percentage of amino acid homology between corresponding regions of human NREBP and mouse NREBP is indicated.

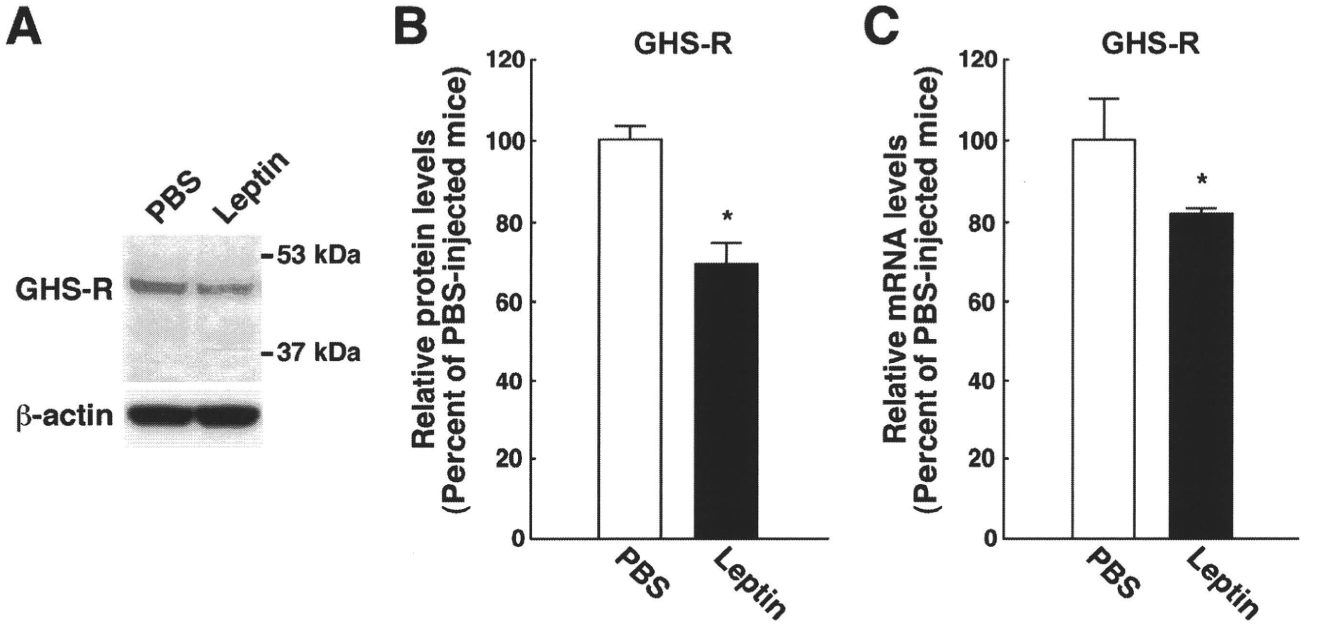

FIGURE 3. **The effect of leptin on the expression of GHS-R in the hypothalamus of *ob/ob* mice.** *A*, Western blot analysis of GHS-R in the hypothalamus of PBS- or leptin-injected *ob/ob* mice ($n = 4$ per group). Lysates prepared from the hypothalamus of PBS- or leptin-injected *ob/ob* mice were separated by SDS-PAGE and immunoblotted with anti-GHS-R antibody. The blots were then stripped and reprobed with anti-β-actin antibody to ensure equal loading of proteins. Apparent molecular masses are indicated on the *right*. *B*, quantitative analysis of the protein expression of GHS-R in the hypothalamus of PBS- (*white bar*) or leptin-injected (*black bar*) *ob/ob* mice. The band intensities of GHS-R were normalized with the band intensities of β-actin and are shown as a percentage relative to the intensities of PBS-injected mice in the bar graphs. *C*, expression of GHS-R mRNA in the hypothalamus of PBS- or leptin-injected mice ($n = 3$ per group). Quantitative real-time PCR was performed by using mRNA prepared from the hypothalamus of PBS- (*white bar*) or leptin-injected (*black bar*) *ob/ob* mice. Data represent the means ± S.E. *, $p < 0.05$ Student's *t* test.

log no. sc-20748, Santa Cruz Biotechnology), rabbit anti-leptin receptor antibody (diluted at 1:500, catalog no. 07–096, Upstate Biotechnology), or rabbit antiphospho-AMP-activated protein kinase α (AMPKα) antibody (diluted at 1:500; Cell Signaling Technology, Beverly, MA) at 4 °C for 16 h, followed by incubation with HRP-conjugated donkey anti-rabbit IgG (diluted at 1:4,000, GE Healthcare). Labeled proteins were detected with chemiluminescence using ECL detection reagent (GE Healthcare) according to the manufacturer's instructions. The membranes were exposed to Hyperfilm ECL (GE Healthcare) for an appropriate period. Then the blotted membranes were stripped in 0.25 M glycine, pH 2.5, at room temperature for 10 min and incubated with mouse anti-β-actin antibody (diluted at 1:10,000; Sigma) or rabbit anti-AMPKα antibody (diluted at 1:500; Cell Signaling Technology) at 4 °C for 16 h, followed by incubation with HRP-conjugated donkey anti-rabbit IgG (diluted at 1:4,000, GE Healthcare) or HRP-conjugated donkey anti-mouse IgG (diluted at 1:20,000, Jackson ImmunoResearch Laboratories) at room temperature for 1 h. The specificity of rabbit anti-GHS-R antibody for Western blot analysis was confirmed by using the hypothalamus of GHS-$R^{-/-}$ mice (supplemental Fig. S1*C*).

Quantitative Real-time PCR—Quantitative real-time PCR was performed with some modifications as described previously (24). Briefly, at 3 h after PBS or leptin injection, *ob/ob* mice were deeply anesthetized with diethyl ether, and the brains were quickly removed. Total RNA was extracted from mediobasal hypothalami as described above. The cDNA from the total RNA was synthesized with TaqMan reverse transcription reagents (Applied Biosystems, Foster City, CA). The following TaqMan gene expression assays (Applied Biosystems) were used: NREBP (Mm00490912_m1), GHS-R (Mm00616415_m1), and 18 S (Hs99999901_s1). Quantitative real-time PCR for each gene was performed using StepOnePlus real-time PCR system (version 2.0, Applied Biosystems) and TaqMan gene expression master mix (Applied Biosystems). The PCR amplification protocol was 50 °C for 2 min, 95 °C for 10 min, and then 40 cycles of 95 °C for 15 s and 60 °C for 1 min. The relative abundance of transcripts was normalized by the expression of 18 S mRNA and analyzed using ΔΔCT method.

Statistical Analysis—Results were shown as means ± S.E. Statistically significant differences for the results from Western blot analysis of pAMPKα and AMPKα in GT1-7 cells were determined by analysis of variance followed by a post hoc Bonferroni test. All other results were analyzed by a Student's *t* test. The criterion for statistical significance was $p < 0.05$.

RESULTS

Identification of Mouse NREBP—To identify the novel genes induced by leptin in the hypothalamus, we performed cDNA subtraction based on selective suppression of PCR using mRNAs from the forebrain of leptin-deficient *ob/ob* mice at 1 h after intravenous injection of PBS or mouse leptin. We chose at random 100 clones in the subtractive library, sequencing their inserts to identify and exclude redundant clones. Inducibility of the genes encoded by the inserts was validated by Northern blot analysis, using the insert as a probe (data not shown). Among them, a gene encoded by a clone 1–42 insert was the mouse homolog of human NREBP. Mouse NREBP consisted of 2281 amino acids and showed 78% homology to human NREBP at the amino acid level. The important domains, Lys-rich, Pro-rich, and Ser/Arg domains, were well preserved between

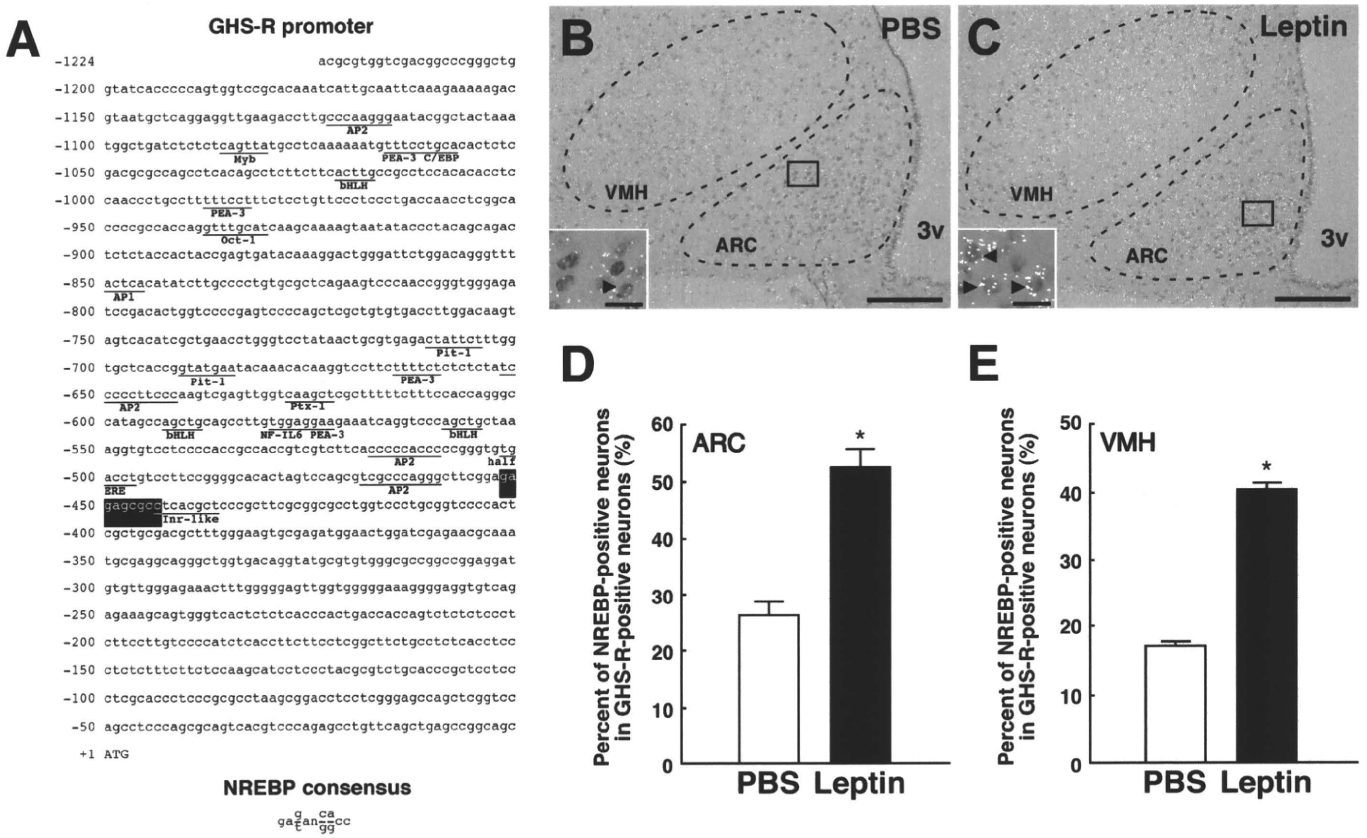

FIGURE 4. **The possibility of a repressive effect of NREBP on the promoter activity of GHS-R.** *A*, optimal NREBP binding sites in the promoter region of GHS-R. The GHS-R promoter region contains a consensus sequence of NRE (from −452 to −444), as shown by the *black box*. *Underlined* sequences indicate the putative binding sites for transcription factors or the initiator-like sequence. *B* and *C*, colocalization of NREBP mRNA and GHS-R in the hypothalamus of PBS- (*B*) or leptin-injected (*C*) *ob/ob* mice ($n = 4$ per group). The *boxed* regions indicated in *B* and *C* are shown at a higher magnification in each *inset*. *Arrowheads* indicate GHS-R-positive neurons (*brown*) with signals for NREBP mRNA (*white dots*). The arcuate nucleus and VMH are shown by the *dotted lines*. *ARC*, arcuate nucleus; *3v*, third ventricle. *Scale bars*, 200 μm; 15 μm in *insets*. *D* and *E*, NREBP- and GHS-R double-positive neurons in PBS- (*white bar*) or leptin-injected (*black bar*) *ob/ob* mice were quantified as the percentage of double-positive neurons in the GHS-R-positive neurons of the arcuate nucleus (*D*) and VMH (*E*). Data represent the means ± S.E. *, $p < 0.05$ Student's *t* test.

human and mouse NREBP (Fig. 1*B*). In addition, the unique repeats, son-a, son-b, and son-c repeats, also showed high homologies in human and mouse: 99% in the son-a, 94% in the son-b, and 93% in the son-c repeat (Fig. 1*B*).

Induction of NREBP by Leptin in Hypothalamus—The intense expression of mouse NREBP mRNA was observed in the brain as well as heart, spleen, liver, skeletal muscle, kidney, and testis (supplemental Fig. S2). To investigate whether leptin up-regulates the expression of NREBP in the hypothalamus, we performed Northern blot analysis using the total RNA from the whole hypothalamus of *ob/ob* mice at 1 h after intravenous injection of PBS or leptin. In the hypothalamus, a major band corresponding to NREBP was detected in PBS-injected *ob/ob* mice (Fig. 2*A*), which increased in the leptin-injected *ob/ob* mice (Fig. 2*A*).

In situ hybridization histochemistry revealed that NREBP mRNA was moderately expressed in some neurons of the brain including the cortex, hippocampus, and piriform cortex in PBS-injected *ob/ob* mice (Fig. 2*B*). However, the expression of NREBP was very weak in the hypothalamus. In addition, the expression of NREBP was increased by leptin exclusively in the hypothalamus at 1 h after leptin administration without affecting NREBP expression in the other regions of the brain (Fig. 2, *B* and *C*).

To determine the localization of leptin-induced NREBP mRNA in the hypothalamus, we measured the number of NREBP-positive cells in the hypothalamus. The number of NREBP-positive cells was increased by leptin in the arcuate nucleus (PBS-injected, 13.7 ± 2.0%; leptin-injected, 23.5 ± 2.7%; Fig. 2, *D–F*) and VMH (PBS-injected, 21.4 ± 2.5%; leptin-injected, 37.5 ± 1.9%; Fig. 2, *D*, *E*, and *G*). There were no differences in the expression of NREBP between PBS-injected or leptin-injected *ob/ob* mice in the other hypothalamic regions: dorsomedial hypothalamic nucleus (PBS-injected, 11.8 ± 2.1%; leptin-injected, 12.2 ± 1.3%), lateral hypothalamic nucleus (PBS-injected, 8.4 ± 1.2%; leptin-injected, 9.2 ± 1.2%), and paraventricular hypothalamic nucleus (PBS-injected, 14.9 ± 3.0%; leptin-injected, 13.7 ± 1.7%).

Suppression of GHS-R Expression by Leptin in Hypothalamus—Next, we explored the transcriptional targets of leptin-induced NREBP in the arcuate nucleus and VMH. Particular attention was paid to GHS-R, which is the ghrelin receptor and mainly expressed in the arcuate nucleus and VMH in the hypothalamus. However, it is unclear whether leptin regulates the expression of GHS-R in the hypothalamus. To test this possibility, we examined the expression of GHS-R at the mRNA and protein levels in the hypothalamus of *ob/ob* mice at 3 h after leptin injection. The expression levels of GHS-R mRNA and protein in the hypothalamus of leptin-injected mice were significantly low compared with those in PBS-injected mice (Fig. 3, *A–C*),

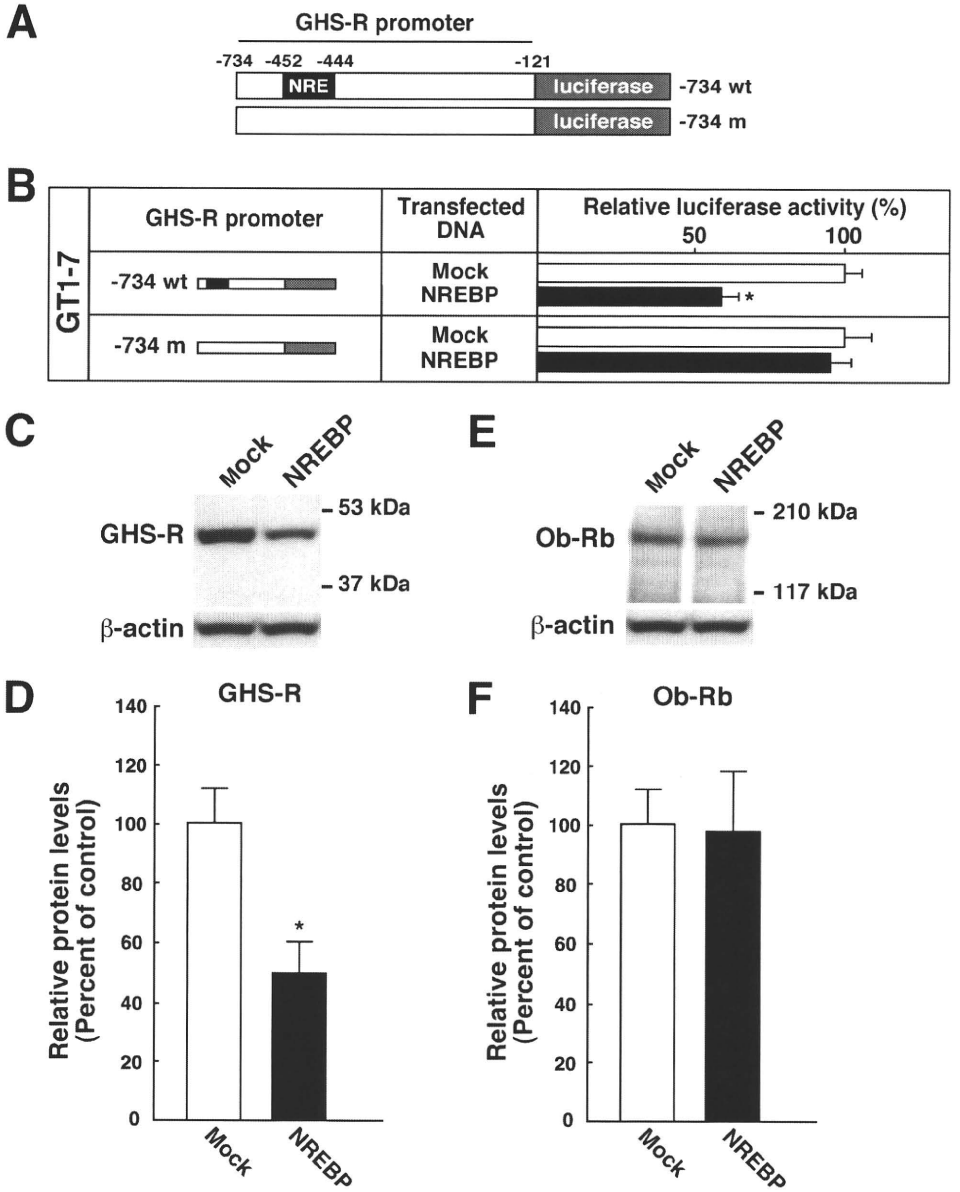

FIGURE 5. **Effects of NREBP on the expression of GHS-R and ob-Rb.** *A*, schematic representation of wild-type GHS-R promoter-luciferase fusion gene (−734 WT) and NRE replacement mutant of GHS-R promoter-luciferase fusion gene (−734 m). *B*, effects of NREBP on the promoter activities of GHS-R in GT1-7 cells. Mock or NREBP (2.5 μg) was transiently transfected with GHS-R promoter-luciferase fusion constract (0.5 μg) and *Renilla* luciferase control reporter plasmid, pRL-TK (0.1 μg) into GT1-7 cells and incubated for 2 days. The promoter activities of GHS-R in mock- (*white bar*) or NREBP-transfected (*black bar*) cells were normalized with *Renilla* luciferase activity and are shown as a percentage relative to the activities of mock-transfected cells. Data represent the means ± S.E. of three independent experiments. *, $p < 0.05$ Student's *t* test. *C–F*, effects of NREBP on the protein expression of endogenous GHS-R (*C* and *D*) or ob-Rb (E and F) in GT1-7 cells. *C* and *E*, Western blot analysis of GHS-R (*C*) or ob-Rb (*E*) in mock- or NREBP-transfected cells. After 3 days of transfection (5.0 μg), cell lysates from mock- (mock) or NREBP-transfected (NREBP) cells were separated by SDS-PAGE and immunoblotted with anti-GHS-R (*C*) or anti-leptin receptor (*E*) antibodies. Then, the blots were stripped and reprobed with anti-β-actin antibody to ensure equal loading of proteins. Apparent molecular masses are indicated on the *right*. *D* and *F*, quantitative analysis of the protein expression of GHS-R after 3 days of transfection with mock or NREBP. The band intensities of GHS-R or ob-Rb in mock- (*white bar*) or NREBP-transfected (*black bar*) cells were normalized with those of β-actin and are shown in the bar graphs as a percentage relative to the intensities of mock-transfected cells. Data represent the means ± S.E. of three independent experiments. *, $p < 0.05$ Student's *t* test.

suggesting that leptin regulates GHS-R expression in the hypothalamus.

Colocalization of NREBP and GHS-R in Arcuate Nucleus and VMH—In the promoter region of human GHS-R (21), there was one NREBP binding sequence, called NRE (25), from −452 to −444 (Fig. 4*A*). In addition, NREBP mRNA was colocalized with GHS-R in the hypothalamus of PBS-injected *ob/ob* mice, and the number of NREBP/GHS-R-double-positive cells was increased by leptin in the arcuate nucleus (PBS-injected, 26.3 ± 5.0%; leptin-injected, 51.9 ± 7.7%; Fig. 4, *B–D*) and VMH (PBS-injected, 17.8 ± 0.6%; leptin-injected, 42.1 ± 0.9% Fig. 4, *B*, *C*, and *E*) at 1 h after the injections. These results strongly suggested that NREBP may play an important role, including transcriptional regulation, in GHS-R-expressing neurons.

Repression of GHS-R Promoter Activity by NREBP in GT1-7 Cells—To examine the effects of NREBP on the promoter activity of GHS-R, we performed luciferase assay using the fusion construct of luciferase reporter and wild-type promoter of GHS-R from −734 to −121 (−734 WT), which contains the NRE from −452 to −444 (Fig. 5*A*). In addition, we used a hypothalamic neuronal cells, GT1-7, to accomplish this aim because GT1-7 cells express GHS-R endogenously. The luciferase activities of GHS-R promoter (−734 WT) were repressed in NREBP-transfected GT1-7 cells compared with those in mock-transfected GT1-7 cells (60.7 ± 6.7%; Fig. 5*B*).

To define the effects of NREBP on NRE, we made an NRE replacement mutant in the GHS-R promoter (−734 m; Fig. 5*A*) and performed luciferase assay. In contrast to −734 WT, the luciferase activity of −734 m was not repressed by NREBP in GT1-7 cells (Fig. 5*B*), suggesting that NREBP represses GHS-R promoter activity by binding to NRE.

Decrease of GHS-R Protein by NREBP in GT1-7 cells—To investigate whether the repression of promoter activity of GHS-R by NREBP leads to the decrease of protein expression of GHS-R, we performed Western blot analysis for endogenous GHS-R in mock- or NREBP-transfected GT1-7 cells. The endogenous protein expression of GHS-R was markedly decreased in NREBP-transfected GT1-7 cells compared with that of mock-transfected GT1-7 cells after 3 days of transfection (49.7 ± 10.4%; Fig. 4, *C* and *D*). There were no significant differences in the protein expression of ob-Rb between NREBP-transfected and mock-transfected cells (Fig. 5, *E* and *F*).

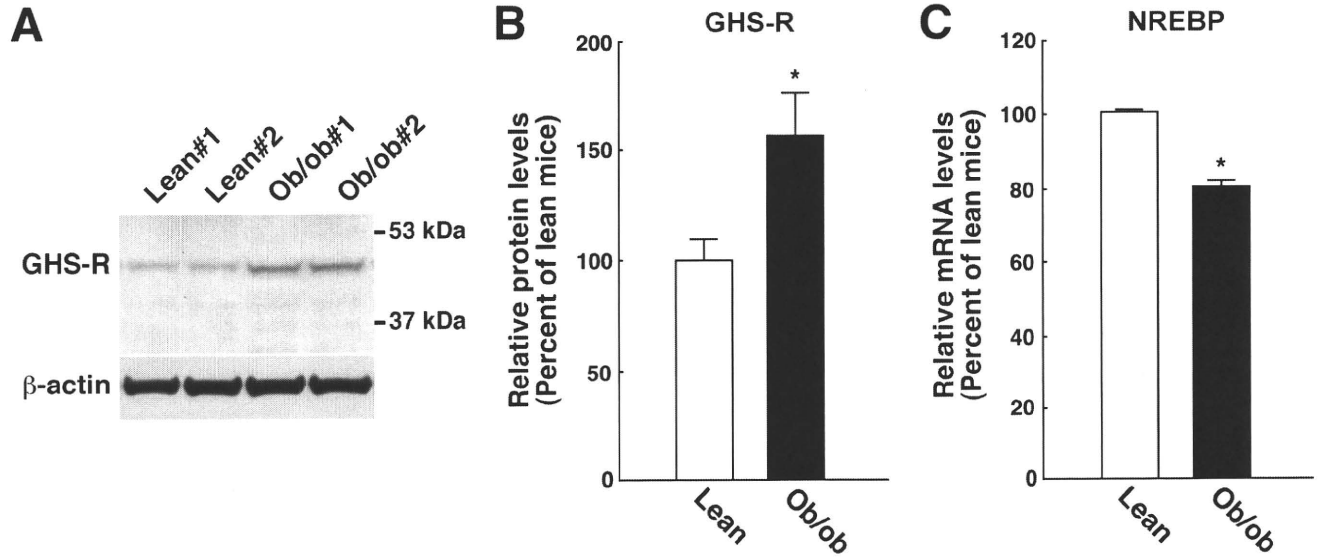

FIGURE 6. **Expression of GHS-R in the hypothalamus of *ob/ob* mice.** *A*, Western blot analysis of GHS-R in the hypothalamus of *ob/ob* mice ($n = 4$ per group). Lysates prepared from the hypothalamus of lean or *ob/ob* mice were separated by SDS-PAGE and immunoblotted with anti-GHS-R antibody. The blots were then stripped and reprobed with anti-β-actin antibody to ensure equal loading of proteins. Apparent molecular masses are indicated on the *right*. *B*, quantitative analysis of the protein expression of GHS-R in the hypothalamus of lean (*white bar*) or *ob/ob* mice (*black bar*). The band intensities of GHS-R were normalized with the band intensities of β-actin and are shown as a percentage relative to the intensities of lean mice in the bar graphs. *C*, expression of NREBP mRNA in the hypothalamus of lean or *ob/ob* mice ($n = 4$ per group). Quantitative real-time PCR was performed by using mRNA prepared from the hypothalamus of lean (*white bar*) or *ob/ob* mice (*black bar*). Data represent the means ± S.E. *, $p < 0.05$ Student's *t* test.

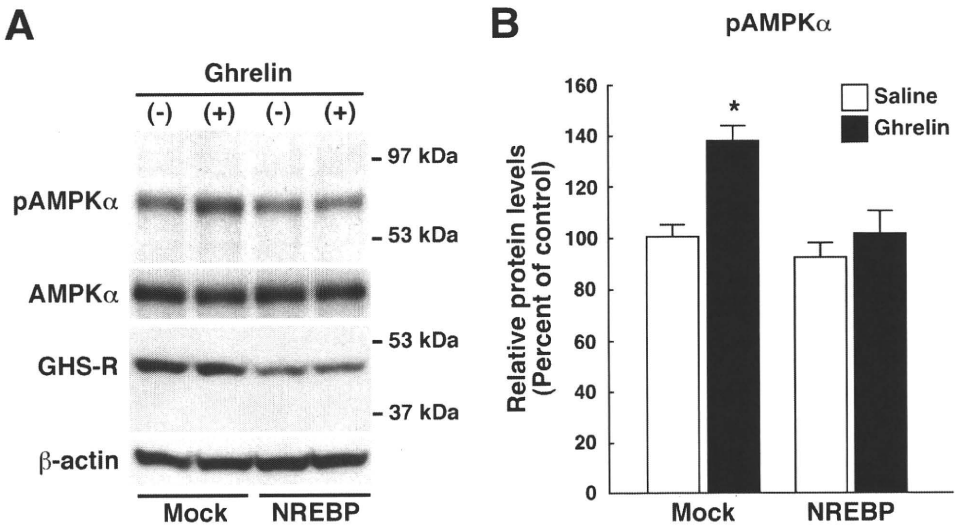

FIGURE 7. **Functional roles of NREBP on the actions of ghrelin.** *A*, inhibitory effects of NREBP on ghrelin-induced AMPK activation in GT1-7 cells. Three days before the experiment, mock or NREBP (5.0 μg) was transiently transfected into GT1-7 cells. The cells were then treated with ghrelin (100 nM) for 5 min. The lysates from these cells were separated by SDS-PAGE and immunoblotted with the anti-pAMPKα or anti-GHS-R antibodies. The blots were stripped and reprobed with anti-AMPKα or anti-β-actin antibody. Apparent molecular masses are indicated on the *right*. *B*, quantitative analysis of the activation of AMPK. The band intensities of pAMPKα of saline- (*white bars*) or ghrelin-treated (*black bars*) cells were normalized with the band intensities of AMPKα and are shown in the bar graphs as a percentage relative to the intensities of mock-transfected saline-treated cells. Data represent the means ± S.E. of three independent experiments. *, $p < 0.05$ analysis of variance followed by post hoc Bonferroni test.

Expression of GHS-R and NREBP in Hypothalamus of ob/ob Mice—To test the effects of leptin-induced NREBP on the expression of GHS-R *in vivo*, we compared the expression of GHS-R between lean and leptin-deficient *ob/ob* mice in the hypothalamus. The expression of GHS-R was increased in the hypothalamus of *ob/ob* mice compared with that of lean mice (Fig. 6, *A* and *B*). In addition, quantitative real-time PCR revealed that the expression of NREBP was decreased in the hypothalamus of *ob/ob* mice compared with that of lean mice (Fig. 6*C*). Thus, the leptin signaling pathway, including NREBP, appear to be important to repress GHS-R expression in the hypothalamus.

Inhibition of Ghrelin-induced AMPK Activation by NREBP in GT1-7 Cells—Recently, hypothalamic AMPK, a key enzyme modulating fatty acid metabolism, is essential for appetite stimulation by ghrelin (26). To determine the effects of NREBP on AMPK activation by ghrelin, we assessed ghrelin-induced phosphorylation of AMPKα in mock- or NREBP-transfected GT1-7 cells. Consistent with Fig. 5 (*C* and *D*), the expression of GHS-R was decreased in NREBP-transfected cells compared with mock-transfected cells (Fig. 7*A*). In mock-transfected GT1-7 cells, ghrelin markedly phosphorylated AMPKα at 5 min after ghrelin treatment (Fig. 7, *A* and *B*). However, phosphorylation of AMPKα was not increased by ghrelin in NREBP-transfected GT1-7 cells (Fig. 7, *A* and *B*).

DISCUSSION

It has been reported that NREBP represses the activities of virus promoters, such as the core promoter of hepatitis B virus (25). Although NREBP expresses in various tissues in human (25) and mouse, the physiological roles of NREBP remain

unclear. In the present study, we identified NREBP as a leptin-induced gene in the mouse hypothalamus. In addition, NREBP repressed the promoter activity of GHS-R via NRE in the hypothalamic neurons. The present study is the first to report the physiological function of NREBP in the hypothalamus.

In the hypothalamic neurons, both transcriptional activities and expression levels of GHS-R were reduced ~45% by NREBP. To confirm whether the ~45% reduction in the expression of GHS-R plays an important role in the signal transduction of ghrelin, we performed functional assays for ghrelin. In hypothalamic neurons, ghrelin activates AMPK by binding to GHS-R (27). In the present study, the overexpression of NREBP completely abolished ghrelin-induced activation of AMPK in a hypothalamic neuronal cell line, GT1-7. Thus, NREBP is important in the regulation of ghrelin signaling, at least in part, through the suppression of GHS-R expression in hypothalamic neurons.

Leptin and ghrelin are inversely correlated in the plasma levels, food intake, and activation of neuropeptide Y neurons (28). Recently, Kohno *et al.* (29) have demonstrated that leptin suppresses ghrelin-induced activation of neuropeptide Y neurons via the phosphatidylinositol 3-kinase- and phosphodiesterase 3-mediated pathway. In addition, the expression of GHS-R is enhanced in the hypothalamus of *fa/fa* rats (30), where normal leptin signaling is ablated by the mutation of leptin receptor, and the GHS-R expression in the hypothalamus is suppressed by leptin treatment (30). However, the molecular mechanisms by which leptin signaling regulates GHS-R expression are largely unknown. In the present study, we also demonstrated that the expression of GHS-R was enhanced in the hypothalamus of *ob/ob* mice. Furthermore, leptin-induced NREBP suppressed the expression and functional roles of GHS-R in the hypothalamus. As the effect of leptin on the expression of GHS-R mRNA takes longer than 2 h (30), suggesting novel gene expression rather than the modulation of signaling pathways, leptin may suppress ghrelin signaling by leptin-induced NREBP.

Both ghrelin gain-of-function and leptin-deficient *ob/ob* mice are hyperphagic and glucose-intolerant (31, 32), suggesting that ghrelin and leptin regulate feeding behavior and glucose metabolism as mutual antagonists. However, it has been reported that the ablation of ghrelin improves the diabetic but not obese phenotype of *ob/ob* mice (33). These findings suggest that factors other than ghrelin are responsible for the development of obesity and hyperphagia in the leptin-deficient *ob/ob* mice. On the other hand, the deficiency of leptin is compensated for by the ghrelin deficiency in the development of diabetes during obesity (33). In the present study, NREBP suppressed ghrelin signaling via the regulation of GHS-R expression. In addition, NREBP was one of the leptin-downstream genes, and its functional abnormality could cause leptin resistance, resulting in insulin resistance. Although further studies are required to determine the precise mechanism of the development of leptin resistance by the mutation of NREBP gene, NREBP can regulate glucose metabolism via linking between leptin and ghrelin signaling and may be an effective target of treatment for diabetes with obesity.

In conclusion, leptin induced the expression of NREBP in the hypothalamus, which suppressed ghrelin signaling via the regulation of GHS-R expression. Our study provides strong evidence for the novel mechanism by which leptin regulates ghrelin signaling in the hypothalamus. Functional abnormality of NREBP may cause leptin resistance, resulting in diabetes with obesity, as obesity is associated with hypothalamic leptin resistance.

Acknowledgments—We thank Dr. Pamela L. Mellon (University of California, La Jolla, CA) for providing the GT1-7 cell line. We also thank Dr. Hidesuke Kaji (Kobe University School of Medicine, Kobe, Japan) for providing the fragment of the 5′-flanking region of the GHS-R gene (−734 to −121) in pGL3-Basic vector. We are grateful to Dr. Dovie Wylie for excellent language support.

REFERENCES

1. Badman, M. K., and Flier, J. S. (2005) *Science* **307,** 1909–1914
2. Coll, A. P., Farooqi, I. S., and O'Rahilly, S. (2007) *Cell* **129,** 251–262
3. Zhang, Y., Proenca, R., Maffei, M., Barone, M., Leopold, L., and Friedman, J. M. (1994) *Nature* **372,** 425–432
4. Banks, W. A., Kastin, A. J., Huang, W., Jaspan, J. B., and Maness, L. M. (1996) *Peptides* **17,** 305–311
5. Tartaglia, L. A., Dembski, M., Weng, X., Deng, N., Culpepper, J., Devos, R., Richards, G. J., Campfield, L. A., Clark, F. T., Deeds, J., Muir, C., Sanker, S., Moriarty, A., Moore, K. J., Smutko, J. S., Mays, G. G., Wool, E. A., Monroe, C. A., and Tepper, R. I. (1995) *Cell* **83,** 1263–1271
6. Schwartz, M. W., Seeley, R. J., Campfield, L. A., Burn, P., and Baskin, D. G. (1996) *J. Clin. Invest.* **98,** 1101–1106
7. Thornton, J. E., Cheung, C. C., Clifton, D. K., and Steiner, R. A. (1997) *Endocrinology* **138,** 5063–5066
8. Kristensen, P., Judge, M. E., Thim, L., Ribel, U., Christjansen, K. N., Wulff, B. S., Clausen, J. T., Jensen, P. B., Madsen, O. D., Vrang, N., Larsen, P. J., and Hastrup, S. (1998) *Nature* **393,** 72–76
9. Mizuno, T. M., and Mobbs, C. V. (1999) *Endocrinology* **140,** 814–817
10. Halaas, J. L., Gajiwala, K. S., Maffei, M., Cohen, S. L., Chait, B. T., Rabinowitz, D., Lallone, R. L., Burley, S. K., and Friedman, J. M. (1995) *Science* **269,** 543–546
11. Farooqi, I. S., Jebb, S. A., Langmack, G., Lawrence, E., Cheetham, C. H., Prentice, A. M., Hughes, I. A., McCamish, M. A., and O'Rahilly, S. (1999) *N. Engl. J. Med.* **341,** 879–884
12. Yang, G., Ge, H., Boucher, A., Yu, X., and Li, C. (2004) *Mol. Endocrinol.* **18,** 1354–1362
13. Chen, K., Li, F., Li, J., Cai, H., Strom, S., Bisello, A., Kelley, D. E., Friedman-Einat, M., Skibinski, G. A., McCrory, M. A., Szalai, A. J., and Zhao, A. Z. (2006) *Nat. Med.* **12,** 425–432
14. Münzberg, H., and Myers, M. G., Jr. (2005) *Nat. Neurosci.* **8,** 566–570
15. Howard, J. K., Cave, B. J., Oksanen, L. J., Tzameli, I., Bjørbaek, C., and Flier, J. S. (2004) *Nat. Med.* **10,** 734–738
16. White, D. W., Zhou, J., Stricker-Krongrad, A., Ge, P., Morgenstern, J. P., Dembski, M., and Tartaglia, L. A. (2000) *Diabetes* **49,** 1443–1450
17. Tamura, S., Morikawa, Y., Miyajima, A., and Senba, E. (2003) *Eur. J. Neurosci.* **17,** 2287–2298
18. Mellon, P. L., Windle, J. J., Goldsmith, P. C., Padula, C. A., Roberts, J. L., and Weiner, R. I. (1990) *Neuron* **5,** 1–10
19. Morikawa, Y., Tamura, S., Minehata, K., Donovan, P. J., Miyajima, A., and Senba, E. (2004) *J. Neurosci.* **24,** 1941–1947
20. Komori, T., Gyobu, H., Ueno, H., Kitamura, T., Senba, E., and Morikawa, Y. (2008) *J. Comp. Neurol.* **511,** 92–108
21. Kaji, H., Tai, S., Okimura, Y., Iguchi, G., Takahashi, Y., Abe, H., and Chihara, K. (1998) *J. Biol. Chem.* **273,** 33885–33888
22. Nakano, Y., Furuta, H., Doi, A., Matsuno, S., Nakagawa, T., Shimomura, H., Sakagashira, S., Horikawa, Y., Nishi, M., Sasaki, H., Sanke, T., and Nanjo, K. (2005) *Diabetes* **54,** 3560–3566

23. Hisaoka, T., Morikawa, Y., Komori, T., Sugiyama, T., Kitamura, T., and Senba, E. (2006) *Eur. J. Neurosci.* **23,** 3149–3160
24. Doi, A., Shono, T., Nishi, M., Furuta, H., Sasaki, H., and Nanjo, K. (2006) *Proc. Natl. Acad. Sci. U.S.A.* **103,** 885–890
25. Sun, C. T., Lo, W. Y., Wang, I. H., Lo, Y. H., Shiou, S. R., Lai, C. K., and Ting, L. P. (2001) *J. Biol. Chem.* **276,** 24059–24067
26. López, M., Lage, R., Saha, A. K., Pérez-Tilve, D., Vázquez, M. J., Varela, L., Sangiao-Alvarellos, S., Tovar, S., Raghay, K., Rodríguez-Cuenca, S., Deoliveira, R. M., Castañeda, T., Datta, R., Dong, J. Z., Culler, M., Sleeman, M. W., Alvarez, C. V., Gallego, R., Lelliott, C. J., Carling, D., Tschöp, M. H., Diéguez, C., and Vidal-Puig, A. (2008) *Cell Metab.* **7,** 389–399
27. Kohno, D., Sone, H., Minokoshi, Y., and Yada, T. (2008) *Biochem. Biophys. Res. Commun.* **366,** 388–392
28. Nogueiras, R., Tschöp, M. H., and Zigman, J. M. (2008) *Ann. N.Y. Acad. Sci.* **1126,** 14–19
29. Kohno, D., Nakata, M., Maekawa, F., Fujiwara, K., Maejima, Y., Kuramochi, M., Shimazaki, T., Okano, H., Onaka, T., and Yada, T. (2007) *Endocrinology* **148,** 2251–2263
30. Nogueiras, R., Tovar, S., Mitchell, S. E., Rayner, D. V., Archer, Z. A., Dieguez, C., and Williams, L. M. (2004) *Diabetes* **53,** 2552–2558
31. Bailey, C. J., Atkins, T. W., Conner, M. J., Manley, C. G., and Matty, A. J. (1975) *Horm. Res.* **6,** 380–386
32. Bewick, G. A., Kent, A., Campbell, D., Patterson, M., Ghatei, M. A., Bloom, S. R., and Gardiner, J. V. (2009) *Diabetes* **58,** 840–846
33. Sun, Y., Asnicar, M., Saha, P. K., Chan, L., and Smith, R. G. (2006) *Cell Metab.* **3,** 379–386

FEBS Letters 584 (2010) 1503–1508

ELSEVIER

FEBS Letters

journal homepage: www.FEBSLetters.org

Ghrelin inhibits insulin secretion through the AMPK–UCP2 pathway in β cells

Ying Wang [a], Masahiro Nishi [b,*], Asako Doi [a], Takeshi Shono [a], Yasushi Furukawa [a], Takeshi Shimada [a], Hiroto Furuta [a], Hideyuki Sasaki [a], Kishio Nanjo [a]

[a] The First Department of Medicine, Wakayama Medical University, Wakayama, Japan
[b] Department of Metabolism and Clinical Nutrition, Wakayama Medical University, Wakayama, Japan

ARTICLE INFO

Article history:
Received 29 December 2009
Revised 22 February 2010
Accepted 27 February 2010
Available online 3 March 2010

Edited by Robert Barouki

Keywords:
Ghrelin
AMP-activated protein kinase
Uncoupling protein 2
Insulin secretion

ABSTRACT

Ghrelin inhibits insulin secretion partly via induction of IA-2β. However, the orexigenic effect of ghrelin is mediated by the AMP-activated protein kinase (AMPK)–uncoupling protein 2 (UCP2) pathway. Here, we demonstrate that ghrelin's inhibitory effect on insulin secretion also occurs through the AMPK-UCP2 pathway. Ghrelin increased AMPK phosphorylation and UCP2 mRNA expression in MIN6 insulinoma cells. Overexpression or downregulation of UCP2 attenuated or enhanced insulin secretion, respectively. Furthermore, AMPK activator had a similar effect to ghrelin on UCP2 and insulin secretion in MIN6 cells. In conclusion, ghrelin's inhibitory effect on insulin secretion is partly mediated by the AMPK-UCP2 pathway, which is independent of the IA-2β pathway.

1. Introduction

Ghrelin, the only circulating orexigenic hormone, was first identified in rat stomach as an endogenous ligand of growth-hormone secretagogue receptor (GHSR) [1]. Although ghrelin is mainly produced and secreted from the stomach [1], pancreas also express ghrelin [2,3] and GHSR [4], as well as the pancreatic β cell line MIN6 cells [5]. In addition, ghrelin concentration is eight times higher in pancreatic veins than in pancreatic artery [6], suggesting that ghrelin is produced and released from islet cells and might act on β cells via autocrine and/or paracrine manner.

Besides modulating energy homeostasis by increasing food intake, body weight and adiposity [7,8], ghrelin was also suggested affecting pancreatic β cell function. Administration of ghrelin resulted in a decrease in plasma insulin and an increase in plasma glucose levels [9]. Overexpression of ghrelin led to inhibition of glucose-stimulated insulin secretion (GSIS) and deleting the gene of ghrelin or GHSR resulted in lower blood glucose [10] in mice. We have reported that ghrelin inhibited insulin secretion via inducing IA-2β [5]. But the intrinsic mechanism of this has not been investigated sufficiently.

AMP-activated protein kinase (AMPK) plays an important role in glucose homeostasis. It is well known that activation of AMPK suppresses GSIS in β cell lines [11] and isolated islets [12]. Ghrelin regulates AMPK activity in various tissues in a tissue-specific manner [13–15]. However, there is no report about how ghrelin affect AMPK activity in β cells till now.

Ghrelin also enhanced uncoupling protein 2 (UCP2) expression in the hypothalamus [13], liver [14] and white adipose tissue [8]. The orexigenic effect of ghrelin on the hypothalamus was demonstrated to be a UCP2-dependent action via AMPK [13]. Ghrelin-deficient mice showed reduced UCP2 mRNA expression and enhanced GSIS [16]. Overexpression of UCP2 in rat islets decreased insulin secretion [17]. Gonzalez-Barroso et al. reported an impaired activity of UCP2 mutants which was related with human congenital hyperinsulinism [18]. Therefore, ghrelin may affect insulin secretion through AMPK-UCP2 pathway.

2. Materials and methods

2.1. Cell culture and reagents

MIN6 cells were maintained in DMEM containing 25 mmol/l glucose, 10% FBS, and antibiotics (Invitrogen, Carlsbad, CA) at

Abbreviations: AICAR, 5-aminoimidazole-4-carboxamide-1-β-D-ribofuranoside; AMPK, AMP-activated protein kinase; GHSR, growth-hormone secretagogue receptor; GSIS, glucose-stimulated insulin secretion; KRBH, Krebs–Ringer bicarbonate–Hepes buffer; PPAR, peroxisome proliferator-activated receptor; PGC-1α, PPAR-γ coactivator-1-alpha; QT-PCR, quantitative real-time PCR; ROS, reactive oxygen species; siRNA, short-interfering RNA; UCP2, uncoupling protein 2

* Corresponding author. Address: Department of Metabolism and Clinical Nutrition, Wakayama Medical University, 811-1 Kimiidera, Wakayama 641-8509, Japan. Fax: +81 73 445 9436.
E-mail address: mnishi@wakayama-med.ac.jp (M. Nishi).

0014-5793/$36.00
doi:10.1016/j.febslet.2010.02.069

37 °C in 5% CO_2. Ghrelin (acylated form) and desacyl-ghrelin were bought from Peptide Ins. (Osaka, Japan). 5-Aminoimidazole-4-carboxamide-1-β-D-ribofuranoside (AICAR) was purchased from Sigma (St. Louis, MO). Antibodies for phospho-AMPK and total AMPK were obtained from Cell Signaling Technology (Danvers, MA).

2.2. Plasmid construction, RNA interference and transfection

Plasmids encoding mouse IA-2β were constructed as described elsewhere [5]; full length UCP2 clone obtained from the cDNA of MIN6 cells was subcloned into the plasmid pcDNA 3.1 (Invitrogen) at the EcoRI–NotI sites. Constructed plasmids were transfected to MIN6 cells using FuGENE6 Transfection Reagent (Roche Diagnostics, Mannheim, Germany). The pcDNA 3.1 vector was used as control. Short-interfering RNA (siRNA) of UCP2 was obtained from QIAGEN (Valencia, CA) and transfected into MIN6 cells by RNAiFect Transfection Reagent (QIAGEN). Negative-control siRNA (accompaniment to RNAiFect) was used as control.

2.3. RT-PCR and quantitative PCR

Total RNA derived from MIN6 cells was reverse-transcribed into cDNA and expression levels of UCP2 and IA-2β mRNA were analyzed by quantitative real-time PCR (QT-PCR) as described before [5]. Primer pairs and FAM-conjugated probes for UCP2 were purchased from Applied Biosystems (Assay ID: Mm00627599_ml). Data were calculated as copy number of each mRNA relative to ARP as an internal control.

2.4. Western blot analysis and AMPK activity

Cultured cells were washed twice with ice-cold PBS and resuspended immediately in lysis buffer containing 1% Non-diet P-40, 140 mmol/l NaCl, 20 mmol/l Tris–HCl (pH8.0), 1 mmol/l $MgCl_2$, 1 mmol/l $CaCl_2$, 1 mmol/l DTT, 10% glycerol, 0.5 mmol/l Na_3VO_4, 20 mmol/l pyrophosphate Na, 1 mmol/l PMSF, 5 mmol/l NaF, 1 mmol/l aprotinin, 4 mmol/l leupeptin, 5 mmol/l pepstatin. Protein content in the lysate was measured using the Bio-Rad Protein Assay kits (Bio-RAD, Hercules, CA). Protein samples (25 μg) were subjected to SDS–PAGE and transferred to nitrocellulose membrane then immunoblotted by using the phospho-AMPK and total AMPK antibodies. The proteins bound to antibodies were detected using horseradish peroxidase-conjugated anti-rabbit IgG (Biosource Int., Camarillo, CA) and visualized by using enhanced chemiluminescence detection system (MILLIPORE, Billerica, MA).

AMPK activity in the samples was assessed using the AMPK kinase assay kit (Cyclex, Nagano, Japan) according to the manufacturer's instructions.

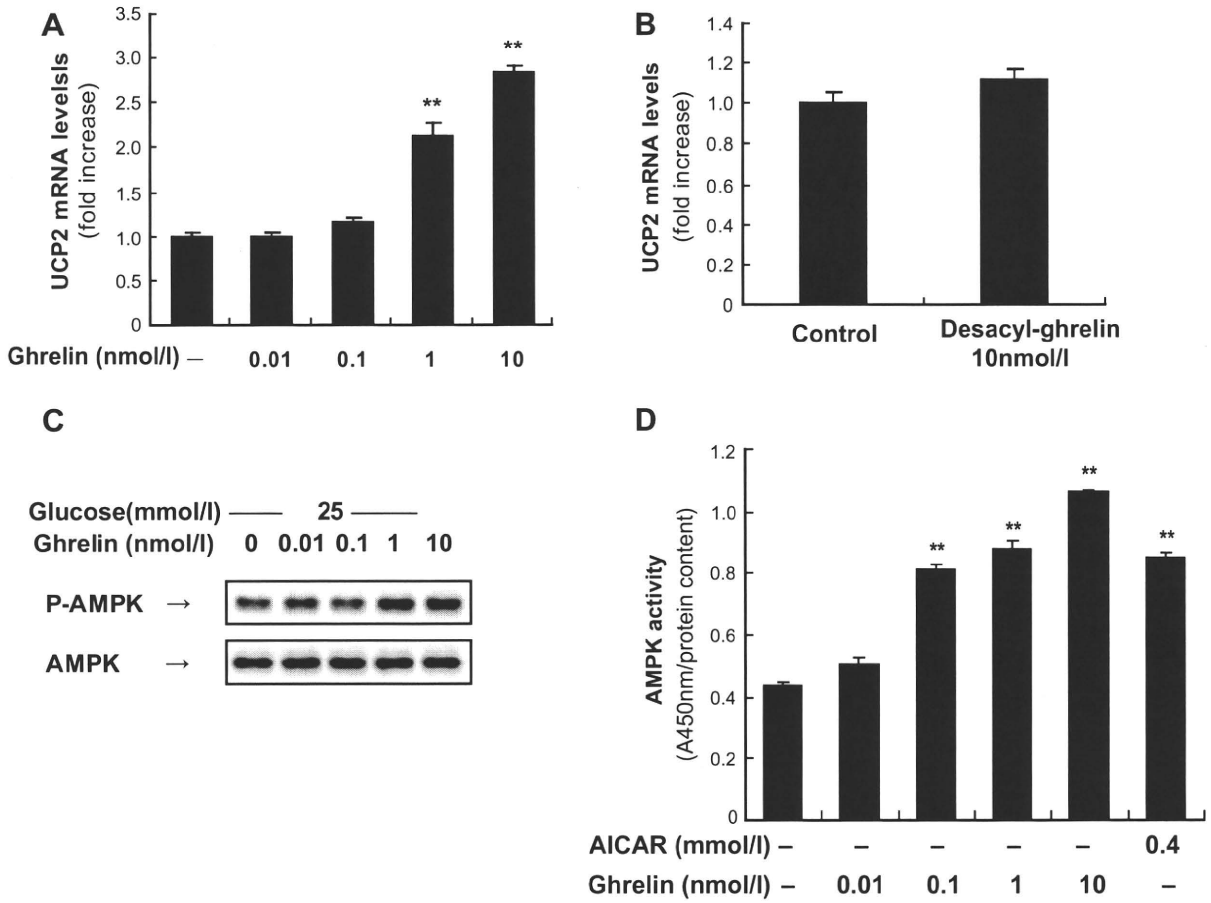

Fig. 1. Effect of ghrelin on UCP2 expression and AMPK activity in MIN6 cells. MIN6 cells were incubated 1 h under the following conditions: (A, C and D) with 0, 0.01, 0.1, 1, 10 nmol/l ghrelin; (B) with or without 10 nmol/l desacyl-ghrelin. (A and B) UCP2 mRNA expression levels were quantified by QT-PCR and expressed as fold increase relative to the values observed with cells that were not stimulated by ghrelin or desacyl-ghrelin. (C) Expression of phospho-AMPK (P-AMPK) and total AMPK (AMPK) were detected by Western blot analysis. The data presented is representative of three independent experiments. (D) AMPK activity was measured by AMPK kinase assay kit and expressed as absorbance at 450 nm and normalized to the protein content of the samples. All values are expressed as means ± S.E. of three independent experiments ($n = 6–12$, $^{*}P < 0.05$; $^{**}P < 0.01$ versus without ghrelin or desacyl-ghrelin).

2.5. Insulin secretion assay and insulin ELISA

The GSIS experiments were carried out as described before [5]. In short, MIN6 cells were incubated with indicated concentrations of glucose in the presence or absence of 10 nmol/l ghrelin or 0.4 mmol/l AICAR for one hour. Insulin content in the supernatant was quantified by an ELISA kit (Linco Research, St. Charles, MO) and normalized by the protein contents of the cell lysate. Data were expressed as ng/mg protein. To study the effect of UCP2 on insulin secretion, MIN6 cells were transfected with pcDNA3.1 UCP2 or UCP2 siRNA and the control vector or control siRNA 24hours before glucose and ghrelin stimulation.

2.6. Statistical analysis

Data are expressed as means ± S.E. for at least three independent experiments in duplicates. Variances in different groups were analyzed by Student's *t*-test or one-way ANOVA for unpaired comparisons. *P* value <0.05 was accepted as significant.

3. Results

3.1. Ghrelin upregulates UCP2 and activates AMPK in MIN6 cells

After the administration of ghrelin for 1 h at high glucose condition, UCP2 mRNA expression levels in MIN6 cells were upregulated dose-dependently (Fig. 1A). However, desacyl-ghrelin did not show any effect on UCP2 (Fig. 1B). Our data are consistent with the view that the acylation is essential for the bioactivity of ghrelin [1]. Ghrelin treatment also induced AMPK phosphorylation (Fig. 1C) as well as AMPK activity (Fig. 1D).

3.2. Effect of UCP2 overexpression or downregulation on insulin secretion

Overexpression of UCP2 attenuated GSIS in MIN6 cells with little or no effect on basal insulin secretion (Fig. 2A). Administration of ghrelin to the cells transfected with UCP2 for 1 h seemed to decrease GSIS further, but without statistical significance (Fig. 2B). On the other hand, downregulation of UCP2 by siRNA technique augmented GSIS in MIN6 cells and abolished ghrelin's inhibitory effect on GSIS (Fig. 2C).

3.3. AICAR elevates UCP2 expression and inhibits GSIS in MIN6 cells

Administration of AICAR (AMPK activator) for 1 h increased UCP2 mRNA expression levels dose-dependently (Fig. 3A), suggesting that AMPK might act upstream of UCP2 to mediate the effect of ghrelin on UCP2. AICAR suppressed the insulin secretion that was induced by 22.2 mmol/l glucose but left the basal insulin secretion intact (Fig. 3B), mimicking the effect of ghrelin. Administration of AICAR and ghrelin together to MIN6 cells decreased GSIS further in contrast to AICAR ($P < 0.05$) or ghrelin (not statistical significant) alone (Fig. 3C). Thus AMPK activation by ghrelin might play a role in the inhibitory effect of ghrelin on insulin secretion by lying between ghrelin and UCP2 and acting as a signal transmitter.

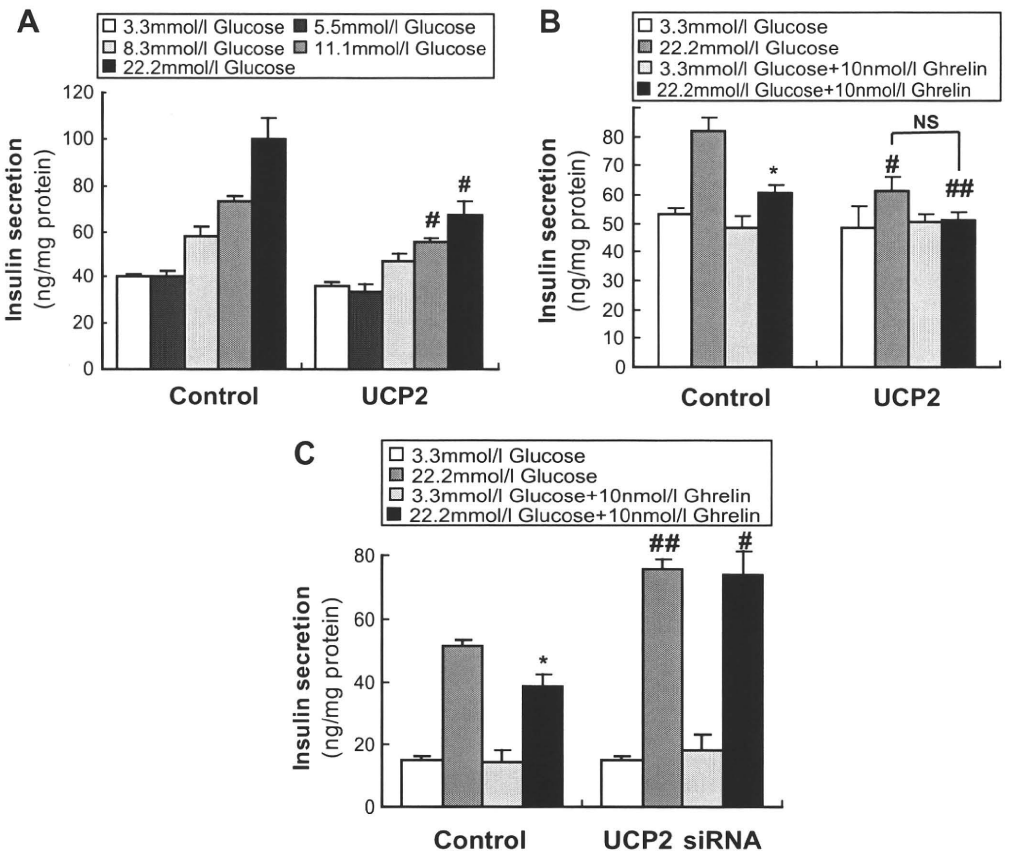

Fig. 2. Effect of UCP2 overexpression or downregulation on insulin secretion. (A and B) MIN6 cells transfected with constructed plasmid, pcDNA3.1 UCP2, or control vector were treated 1 h with (A) indicated concentrations of glucose (3.3, 5.5, 8.3, 11.1, 22.2 mmol/l); (B) 3.3 or 22.2 mmol/l glucose containing 10 nmol/l ghrelin or not. (C) MIN6 cells transfected with UCP2 siRNA or control siRNA were treated as described in (B). Insulin secreted into the medium was measured and normalized to the protein content of cell lysate. All values are expressed as means ± S.E. of three independent experiments ($n = 6–12$, $^{*}P < 0.05$ versus without ghrelin at the same condition. $^{\#}P < 0.05$; $^{\#\#}P < 0.01$ versus control vector or control siRNA transfection without ghrelin).

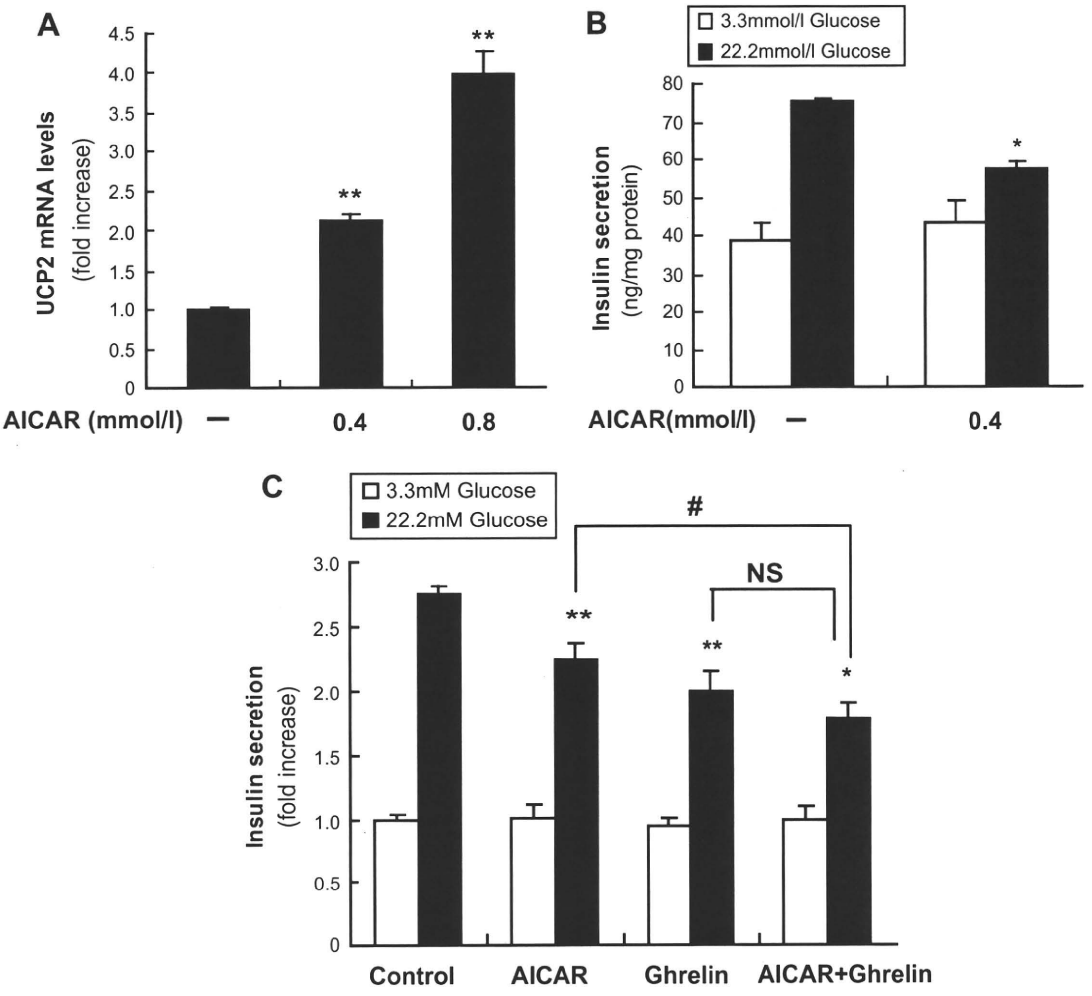

Fig. 3. Effect of AMPK activation by AICAR on UCP2 mRNA expression levels and insulin secretion. (A) UCP2 mRNA expression levels in MIN6 cells treated with AICAR (0, 0.4, 0.8 mmol/l) for 1 h. Data were expressed as fold increase relative to those observed without AICAR. (B) Insulin secretion in MIN6 cells treated 1 h with or without 0.4 mmol/l AICAR in the presence of 3.3 or 22.2 mmol/l glucose. Data were normalized to the protein content of cell lysate and expressed as ng/mg protein. (C) Insulin secretion in MIN6 cells treated with 0.4 mmol/l AICAR and 10 nmol/l ghrelin for 1 h. Data were expressed as fold increase relative to that obtained from the control cells incubated in 3.3 mmol/l glucose. All values are expressed as means ± S.E. of three independent experiments ($n = 6–9$, $^{*}P < 0.05$; $^{**}P < 0.01$ versus control not treated with AICAR and ghrelin. $^{\#}P < 0.05$ versus AICAR).

3.4. Interaction among AMPK, UCP2 and IA-2β

As we have reported that ghrelin inhibits GSIS via inducing IA-2β [5], we assumed that a crosstalk existed between the AMPK–UCP2 pathway and IA-2β pathway. But AMPK activation by AICAR failed to change IA-2β mRNA expression levels (Fig. 4A) in MIN6 cells. Moreover, overexpression of UCP2 did not affect IA-2β mRNA expression levels (Fig. 4B), and vice versa (Fig. 4C). These data suggest that there is not interaction between the two pathways.

4. Discussion

This study was designed to investigate the molecular mechanism of ghrelin's inhibitory effect on GSIS in pancreatic β cells. In this study, we found that ghrelin (acylated form) activates AMPK–UCP2 pathway in MIN6 cells. Furthermore, this pathway modulates GSIS. Therefore, this pathway plays a part in the inhibitory effect of ghrelin on insulin secretion.

Recently, UCP2 was suggested to regulate insulin secretion in many reports. We reported that the UCP2 promoter polymorphism −866G/A was related with GSIS and requirement of insulin therapy in Japanese type 2 diabetes [19]. Here by modulating UCP2 expression levels, we showed that UCP2 is closely related with insulin secretion and interfere with ghrelin's impact to MIN6 cells.

UCP2-deficient mice had higher islet ATP levels and increased GSIS [20]. On the contrary, overexpression of UCP2 in β cells abolished the inhibitory effect of glucose on KATP channel activity and diminished the glucose-stimulated increase of cytosolic Ca^{2+} concentration and insulin secretion [21].

AMPK activation increases the expression of UCP2 in liver [22], skeletal muscle [23], hypothalamus [13], and endothelial cells [24]. Here we found that activation of AMPK by AICAR upregulates UCP2 mRNA expression in MIN6 cells as well.

The mechanism through which AMPK increases UCP2 expression remains unclear. Peroxisome proliferator-activated receptor (PPAR) family, PPAR-α and PPAR-γ coactivator-1-alpha (PGC-1α) which have been described as regulators of mitochondrial biogenesis may be the possible mediators. It was suggested recently that the NAD^{+}-dependent type III deacetylase SIRT1 might lie between AMPK and PGC-1α [25]. On the other hand, reactive oxygen species (ROS) may be another choice. AMPK activation in β cells increased production of ROS, and increased ROS then promote UCP2 transcription and activity [13,26].